2014

Physico-Chemical Properties of Green Leaf Volatiles

Harsha Satyanarayana Vempati
Louisiana State University and Agricultural and Mechanical College

PHYSICO-CHEMICAL PROPERTIES OF GREEN LEAF VOLATILES

A Thesis

Submitted to the Graduate Faculty of the
Louisiana State University and
Agriculture and Mechanical College
in partial fulfillment of the
requirements for the degree of
Master of Science in Chemical Engineering

in

Cain Department of Chemical Engineering

by
Harsha Satyanarayana Vempati
B.S., Georgia Institute of Technology, 2012
December 2014

ACKNOWLEDGEMENTS

I would like to thank my advisor, Dr. Kalliat T. Valsaraj, for his unmatched technical insight and vision. His knowledge and dedication have inspired and challenged me to become a better researcher and engineer. I would also like to thank my committee members, Dr. Francisco Hung and Dr. Louis Thibodeaux, for their time.

I would also like to thank the two extraordinarily knowledgeable and patient post-doctoral researchers I've had the privilege of working under. Dr. Franz Ehrenhauser had an inspiring breadth of practical knowledge which helped me greatly. Dr. Mickael Vaitilingom's encouragement, enthusiasm, and continuous willingness to teach were vital to this work.

Funding for this work came from the National Science Foundation under Award Number AGS-1106559. Our collaborators from University of California, Davis, Dr. Cort Anastasio, Dr. Nicole Richards-Henderson, and Richie Kaur have done excellent work.

I am grateful to my wonderful labmates Aubrey Heath, Paria Avij, and Amie Hansel for their assistance, support, and readiness to share knowledge. Finally, I would finally like to thank my friends and family for their unconditional love and support.

TABLE OF CONTENTS

ABSTRACT

Green Leaf Volatiles (GLVs) is a class of vegetation emissions whose release is greatly enhanced in the event of thermal or mechanical stress. These oxygenated hydrocarbons that have been identified as a potential source of Secondary Organic Aerosols (SOA) via aqueous oxidation. The physico-chemical properties of GLVs are vital to understanding their fate and transport in the atmosphere, but few experimental data are available. We studied the aqueous solubility, 1-Octanol/Water Partition Coefficient, and Henry's Constant (K_H) of five GLVs at 25°C: methyl jasmonate, methyl salicylate, 2-methyl-3-buten-2-ol, cis-3-hexen-1-ol, and cis-3-hexenyl acetate. Henry's constant was additionally measured at 30°C & 35°C, and also in the presence of fog water's common ion compounds with ionic strengths of 0.01 M and 1 M. Experimental values when available from literature are presented, as well as estimations using group and bond contribution methods and property-specific correlations. Estimations are compared to the measured values. The large Henry's constant of methyl jasmonate (8091 ± 1121 $M \cdot atm^{-1}$) made it the most significant GLV for aqueous phase photochemistry. The HENRYWIN program's bond contribution method from the Estimation Programs Interface Suite produced the best estimate of the Henry's Constant for GLVs. The best estimate of 1-Octanol/Water Partition Coefficient and Solubility came from correlating an experimental value of one to find the other. The Henry's Constant values were used to determine the air-water and air-surface interface partition coefficients. Calculations using these partition coefficients showed the percentage of mols of four GLVs residing at the air-water interface of a fog droplet is significant compared to the bulk. Finally, the scavenging efficiency is calculated for each GLV indicating aqueous phase processing will be important for MeJa.

CHAPTER 1
INTRODUCTION AND LITERATURE REVIEW

Introduction

Atmospheric waters such as clouds and fog play a vital role in earth's hydrological cycle, routinely covering half of the earth's surface when viewed via satellite imaging (Pruppacher and Jaenicke 1995, Seinfeld et al. 2006). They have an impact on the global radiative budget as well as the atmospheric chemistry. Far from pure water, these cloud and fog waters have been shown to contain a variety of environmental oxidants, particulate matter, and dissolved chemical compounds. These atmospheric aqueous phases are host to a complex multiphase interaction including: partitioning of organic compounds between the gas, aqueous and solid phases, processing of dissolved particle species, and serving as air-water interfaces upon which adsorption and evaporation can occur (Blando and Turpin 2000, Fowler et al. 2009, Herckes et al. 2013). Fog water is especially interesting to study due to its near-ground formation and ensuing potential for interactions with humans and nearby emissions.

The atmosphere contains a complex and shifting mixture of chemicals, some of the most significant are the volatile organic compounds (VOCs). They are interpreted generally as "organic chemical compounds whose composition makes it possible for them to evaporate under normal indoor atmospheric conditions of temperature and pressure." (EPA). The atmospheric gas phase is an important reservoir for VOCs, and while there VOCs are known to be particularly involved in photochemical transformation pathways (Atkinson 2000, Robinson et al. 2007). An estimate of 1300 Tg Carbon·yr^{-1} of total VOCs (Goldstein and Galbally 2007) is emitted into the atmosphere, of which an estimated 1150 Tg C·yr^{-1} has biogenic origins such as ocean or vegetation emissions, with the balance of anthropogenic origin (Guenther et al. 1995). The

biogenic volatile organic compounds (BVOCs) are comprised of: monoterpenes (44%), isoprene (11%), other reactive VOC (ORVOC) (22.5%), and other VOC (OVOC) (22.5%). While monoterpene and isoprene emissions have good estimates, large uncertainties exist for estimates of the latter two categories, and only a portion of VOC emissions in these categories are speciated. By 1987, atmospheric measurements had identified tens of thousands of VOCs in the ORVOC and OVOC categories (Graedel 1978, Graedel 1986) – still only a fraction of those thought to exist - yet only a small portion of them have been studied.

Of the ORVOCs, one of the most significant groups are green leaf volatiles (GLVs), emitted by many plants including: grass, oak, orange, clover, onion, and lettuce (Arey et al. 1991, Kirstine et al. 1998). These oxygenated, low molecular weight hydrocarbons are formed in plants in the bio-catalyzed conversion of the omega-6 fatty acid linoleic acid. (Matsui 2006, Hamilton et al. 2009) and play a role in signaling between plants (Matsui 2006). While healthy plants emit only trace amounts, they are emitted in greatly enhanced quantities if the plant undergoes stress such as mechanical agitation, temperature changes, and animal or insect grazing (Kirstine et al. 1998, Farag and Pare 2002). GLVs have also been shown to have antimicrobial properties and can even limit herbivores by recruiting their carnivorous enemies (Shiojiri et al. 2006). The most prevalent appear to be C_6-oxygenates (Hamilton et al. 2009). Atmospheric mixing ratios for GLVs have been estimated from 100-900 ppt (Williams et al. 2001, Jardine et al. 2010, Kim et al. 2010), a potentially significant portion of the estimated 1-3 ppb (Kesselmeier and Staudt 1999) mixing ratio allotted for ORVOCs.

While the umbrella term GLV covers many compounds and their derivatives, the focus was on five GLVs crucial to the stress response (Arey et al. 1991, Harley et al. 1998, Heiden et al. 1999, Preston et al. 2001): methyl jasmonate (MeJa), methyl salicylate (MeSa), 2-methyl-3-

buten-2-ol (MBO), cis-3-hexen-1-ol (HxO), and cis-3-hexenylacetate (HxAC). While to our knowledge MeJa has not been detected in forests it is emitted in the vapor phase (Preston et al. 2001), and MBO, HxAC, HxO, and MeSa all have been detected over active vegetation. (Williams et al. 2001, Jardine et al. 2010, Kim et al. 2010). Their structures are shown in Figure 1, and their basic properties are shown in Table 1. They have been shown to participate in gas phase reactions with ozone and hydroxyl radicals (Hamilton et al. 2009, Harvey et al. 2014). This is particularly interesting because it hints at their potential to participate in aqueous phase photochemical reactions and form heavier molecular weight products (Richards-Henderson et al. 2014).

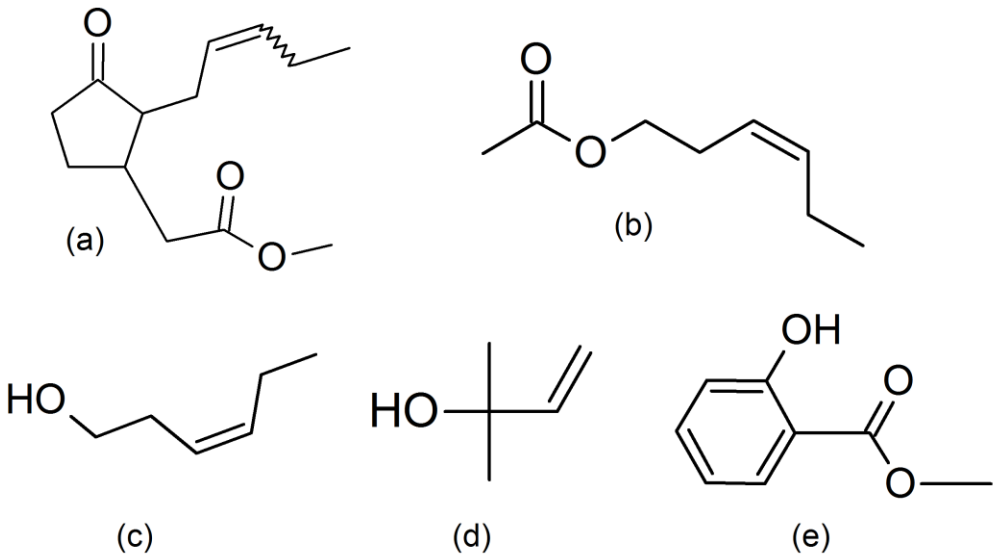

Figure 1. Molecular Structures of (a) methyl jasmonate (MeJa), (b) cis-3-hexenylacetate (HxAC), (c) cis-3-hexen-1-ol (HxO), (d) methyl buten-2-ol (MBO), and (e) methyl salicylate (MeSa)

Table 1. Basic Properties of GLVs.

GLV	CAS Number	Molecular Formula	Molecular Weight [g·mol^{-1}]	Boiling Point [°C]	Density at 25°C [g·mL^{-1}]
MeJa	39924-52-2	$C_{13}H_{20}O_3$	224.3	110	1.03
MeSa	119-36-8	$C_8H_8O_3$	152.15	222	1.174
MBO	115-18-4	$C_5H_{10}O$	86.13	98-99	0.824
HxO	928-96-1	$C_6H_{12}O$	100.16	156-157	0.848
HxAC	3681-71-8	$C_8H_{14}O_2$	142.19	75-76	0.897

Fog Water

Radiation fogs (of the type found in Baton Rouge) are formed when the ground surface cooled by its emission of thermal radiation contacts and cools air supersaturated with water vapor, instigating vapor condensation around nearby particulates. These droplets have approximate diameters of 1-10 μm (Valsaraj 2012). The density of the fog is characterized by its liquid water content, defined as the mass of water in the liquid phase per volume of dry air, which can range from 0.02 to 1 [$g \cdot m^{-3}$] (Seinfeld and Pandis 1998), and in Baton Rouge was measured to be 0.008 – 0.33 [$g \cdot m^{-3}$] (Raja et al. 2009). Samples of fog water have been collected worldwide and have been found to contain significant amounts of organic carbon (1 – 200 mg $C \cdot L^{-1}$ aqueous volume) (Herckes et al. 2013), an estimated 75% of which is dissolved. This dissolved portion includes a substantial amount of speciated carboxylic acids and carbonyls, but often the majority of DOC are unidentified organic molecules (Herckes et al. 2013). Fog droplets also contains solid particles which enter through collision or by becoming the associated nucleation site upon which the fog droplet grows by condensation (Herckes et al. 2013). In addition to organic carbon, fog also contains environmentally generated oxidants like hydroxyl radicals which enter the droplet via the gas phase or are produced inside the droplet from the hydrogen peroxide and other reactive species.

While much of the work regarding kinetics of aqueous phase oxidation reactions has been done in the bulk phase, the reactions of compounds which may reside and react at the air-water interface are less explored. Surface active compounds adsorbed to the air-water interface can be present at the surface in large enough amounts to be considered a “surface phase”, significant numbers of absolute mols relative to the bulk for small aqueous droplets (Valsaraj 2009). Recent molecular dynamics simulations have shown that some GLV orientations occupy a free energy

minimum at the air-water interface (Liyana-Arachchi et al. 2013, Liyana-Arachchi et al. 2013, Liyana-Arachchi et al. 2014). Additionally, surface reactions have been shown to have enhanced reaction rates compared to the bulk (Chen et al. 2006, Richards-Henderson et al. 2014). This can be understood intuitively: a molecule in complete dissolution in the bulk phase has a "cage" of water molecules around it, in an orientation minimizing the Gibbs Free Energy. In order to react with it, an oxidant must diffuse to and through this barrier; a heterogeneous reaction at the air-water interface between adsorbed or only partially dissolved reactants does not face these barriers. Surface active compounds can be detected because they decrease the surface tension of a compound by interrupting the hydrogen bonding at the surface. Measurements show the surface tension of fog water is less than that of pure water (Facchini et al. 2000) indicating the presence of surface active compounds.

Secondary Organic Aerosols

VOCs processing in fog is significant here because it has been shown to lead to the formation of secondary organic aerosol (SOA) (Volkamer et al. 2006, Hallquist et al. 2009, Ervens et al. 2011). SOA is introduced into the atmosphere via chemical reactivity, they differ from primary organic aerosols, which enter the atmosphere directly as dust, ocean salt from sea sprays, volcanic emissions, or industrial anthropogenic emissions (Chin et al. 2009). The formation of SOA inside atmospheric aqueous droplets has been linked to the oxidation of dissolved volatile organic matter (Hallquist et al. 2009, Mentel et al. 2013). The oxidation of DOC in aqueous atmospheric aerosols results not only in the formation of low weight molecular compounds but also in the formation of higher molecular weight products by oligomerisation (Hall and Johnston 2010). These lower volatility products may then partition into the particle phase, or could aggregate and reach a high enough molecular mass to be considered SOA. SOAs

are significant because they affect respiratory health in animals (Mauderly and Chow 2008), reduce visibility, and have a significant yet poorly understood radiative forcing effect (Change 2013). Their complex radiative behavior results from their varied composition and origin – black carbon aerosols absorb radiation, but other organic aerosols reflect it (Kanakidou et al. 2005). Additionally they serve as cloud condensation nuclei (CCN) thus participating in the atmospheric water cycle and indirectly affecting the radiation budget. Their role as CCN gives rise to the so-called fog-smog-fog cycle whereby fog droplets are formed, process VOCs and produce SOA, settle gravitationally then evaporate – leaving behind more aerosols at ground level to serve as new CCN (Munger et al. 1983). While GLVs formation of SOA has been investigated in the gas phase (Hamilton et al. 2009), their role in aqueous phase SOA production has only recently been explored (Richards-Henderson et al. 2014).

Partitioning and Equilibrium Properties

Equilibrium physico-chemical properties allow the determination of the direction and magnitude of the thermodynamic coercion on a molecule in the environment. Upon the formation of a fog droplet, a complex interplay of physical processes begins in and around the newly formed aqueous phase. This is shown in Figure 2 below. The soluble portion of the particulate nucleus begins to dissolve, gases including both VOCs and oxidants from the surrounding air meet the air-water interface and are adsorbed or absorbed, reactions between various dissolved compounds begin, and the droplet itself grows, contracts, and collides with other droplets. The extent of the partitioning of a VOC into each of the three compartments: air, bulk aqueous, and air-water interface at equilibrium is vital to understanding an analyte's environmental fate and thus its potential to produce SOA. The relationships between each of the three compartments are represented by partition coefficients as shown in Figure 3 below.

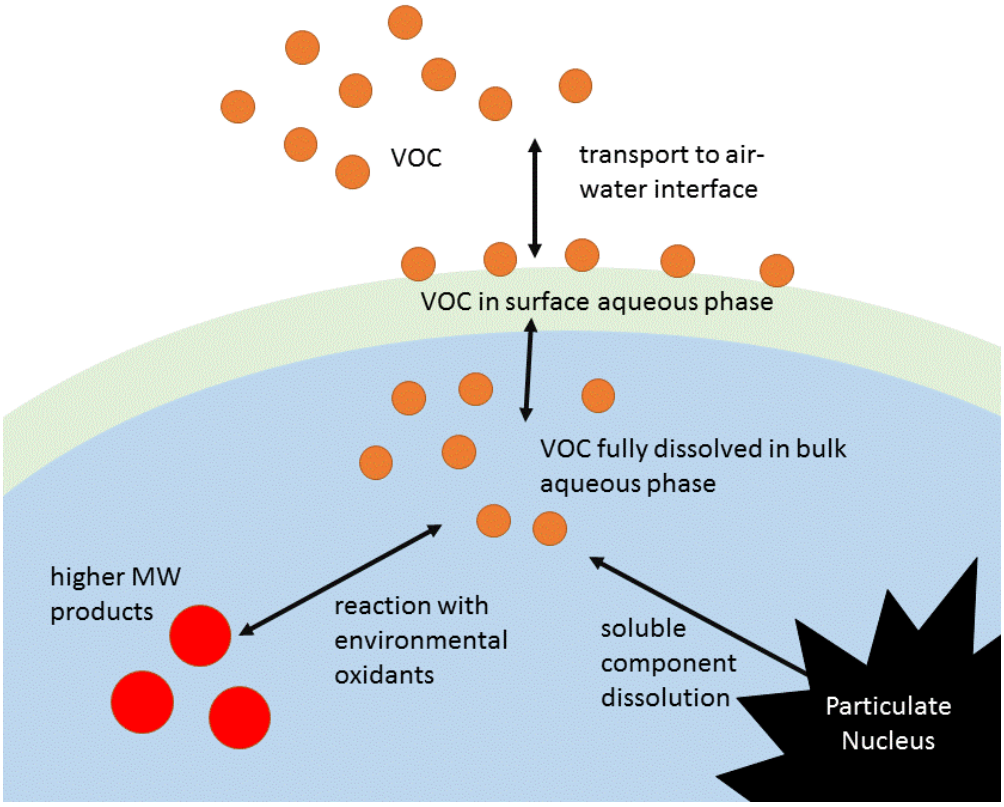

Figure 2. Physical processes occurring in a dispersed aqueous phase.

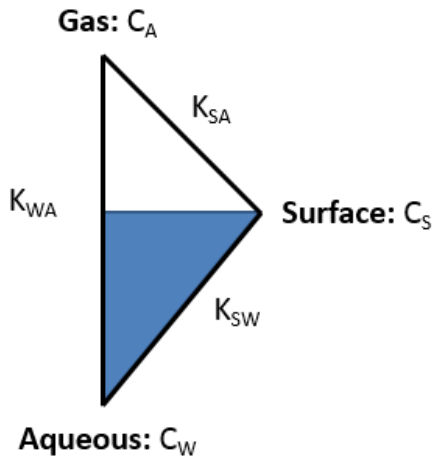

Partition Coefficients are a ratio, naming convention used is $\frac{First\ Subscript}{Second\ Subscript}$

Figure 3. The relationship between the three phase concentrations and their partition coefficients.

The ratio of bulk aqueous concentration C_W to gas phase concentration C_A for an analyte in an air-water system at equilibrium is governed by its Henry's Constant K_H [M/atm], an extremely important parameter in determining the eventual fate of a compound in the environment. Likewise a compound's concentration ratio between the surface to bulk aqueous compartments is given by K_{SW} and its concentration ratio between surface to air compartments is K_{SA}. In this way, if the concentration in one phase of an air-water system is known, the others can be found. A compound's octanol-water partition coefficient $\log(K_{OW})$, defined as the concentration ratio of an analyte in a system of mutually saturated octanol and water, is another important partition measure, indicating an analyte's hydrophobicity (Valsaraj 2009). It can be correlated to find soil/water and gas-to-particle partitioning in the atmosphere. Finally a compound's saturated aqueous solubility, S [mM], is an important equilibrium value used to express hydrophilicity and determine the extent to which it is possible for an analyte to partition into the aqueous phase – relevant here because an analyte partitioning into fog may be limited by its solubility S.

Research Objective

This research aims to experimentally determine and evaluate estimations for the physico-chemical properties of the five chosen GLVs, and in doing so elucidate their partitioning behavior and environmental fate. For each chosen GLV, the Henry's Constant K_H at three different temperatures and ionic strengths, their enthalpy and entropy of phase change, and their aqueous solubility were measured. While measured K_H values can be found in the literature for most GLVs, they have been measured only at 25°C in pure water (above the temperature of fog formation). In order to be relevant for environmental conditions of fog formation, K_H must be measured at different temperatures and ionic strengths. Additionally these parameters will be

predicted using prominent estimation methods and software for which GLVs present an excellent test case because they are all multifunctional oxygenated alkenes which may have complex polar character. This work includes: measurements of K_H at various temperatures and ionic strengths, aqueous solubility determination, and estimations of log(K_{OW}), S, and K_H for these five GLVs: methyl jasmonate (MeJa), methyl salicylate (MeSa), 2-methyl-3-buten-2-ol (MBO), cis-3-hexen-1-ol (HxO), and cis-3-hexenylacetate (HxAC).

CHAPTER 2
PHYSICO-CHEMICAL PROPERTY ESTIMATION METHODS

Introduction

As mentioned in Chapter 1, values of physico-chemical properties are vital to understanding the fate and transport of chemicals in the environment. For many compounds of interest, experimentally measured values of these properties are not available, so there exist a variety of methods to estimate them. They can be divided loosely into two categories: quantitative structure property relationships (QSPR), and quantitative physical property relationships (QPPR). Estimations of both types are used not only for smaller functional organic molecules of environmental interest, but also complex, multifunctional molecules and pharmaceutical drugs.

QSPRs are based on the tenet that a compound's thermodynamic properties are the consequence of its atomic makeup and molecular structure. Each molecular attribute in the molecule is assigned a contribution value, and the contributions from all of attributes in a molecule are summed to estimate the desired property. Two main types exist; bond contribution schemes count each individual bond and are applicable to a wide range of compounds, while group contribution methods count only functional groups. Group contribution approaches are generally regarded as more accurate (Staudinger and Roberts 1996), but also more limited because they fail to give a result if a compound contains a functional group which is not in their dataset. Group contributions are also often trained on datasets containing monofunctional compounds so as to isolate and ascertain the effect of a single functional group, and thus can misestimate by neglecting effects of adjacency or a molecule's overall complex polar character. Both can be made more accurate by limiting the training set to compounds of a certain class, at the expense of general usefulness - many environmentally relevant compounds have multiple

functionalities (for instance the GLVs in this paper). In general both group and bond contribution methods will be more inaccurate the more complex the molecule is.

QPPRs correlate separate known or estimated physico-chemical properties such as solubility, or molecular descriptors such as surface area to find the desired property. These can be simple correlations with a known measured property, or large poly-parameter models using a variety of estimated and calculated properties. They can be derived from fundamental thermodynamics or simply reflect an observed correlation. QPPRs also frequently combine molecular structural and functional group or structural properties as in QSPRs with physic-chemical descriptors as found in to estimate a parameter, and thus the division between QSPRs and QPPRs is not definite.

Henry's Constant

Henry's Constant is most easily estimated by taking a vapor pressure to solubility ratio, however neither of these values are available for GLVs, and estimating both to in turn estimate K_H would introduce a large error. Many bond contribution methods exist (Cramer 1980, Cabani et al. 1981, Modarresi et al. 2007), here two prominent and easy to use methods were applied to predict K_H: that of Hine & Mookerjee (1975) (Hine and Mookerjee 1975) and the HENRYWIN program (Meylan and Howard 1991) from the Environmental Protection Agency's Estimation Property Interface Suite (referred to here as HENRYWIN-BOND). HENRYWIN-BOND is based on an updated version of Hine & Mookerjee's original protocol, with an expanded training set and corrections for problematic functional groups. HENRYWIN's group contribution method (HENRYWIN-GROUP) was also used, based exactly on Hine & Mookerjee's original protocol. Two methods combining molecular connectivity indices, group contributions, and polarizability were also used: those of Nirmalakhandan et al. (Nirmalakhandan et al. 1997) and Suzuki et al.

(Suzuki et al. 1992). These methods use information about molecular configuration in their calculations, and are thus able to recognize differences between isomers. While many QPPRs exist for K_H determination (Russell et al. 1992, Abraham et al. 1994, Schüürmann 1995, Dearden and Schüürmann 2003), but they often require unavailable or demanding calculations of molecular parameters to use. Thus, the only QPPR used for K_H determination was SPARC Performs Analytical Reasoning in Chemistry (SPARC) online calculator based on a blend of Linear Free Energy Relationships and Perturbed Molecular Orbital theory (Hilal et al. 2003).

Solubility

Many estimations were performed to obtain the aqueous solubility of GLVs including: EPI Suite's WATERNT bond contribution method (Meylan and Howard 1995), the group contribution method of Marrero & Gani (Marrero and Gani 2002), and SPARC. In addition, the logarithm of solubility log(S) is also commonly estimated by using correlations with either experimentally determined or estimated log(K_{OW}) values. The relation arises by manipulating the fugacity equations of an analyte in solution and octanol, eventually giving Equation 1. (Chiou et al. 1982)

$$\log(K_{OW}) = -\log(S) - \log(\bar{V}_O^*) - \log(\gamma'_O) + \log\left(\frac{\gamma'_W}{\gamma_W}\right) \quad (1)$$

$\bar{V}_O^*$ is the molar volume of octanol saturated with water, γ'_O is the activity coefficient of the solute in octanol saturated with water, γ'_W is the solute activity coefficient in water saturated with octanol, and γ_W is the solute activity coefficient in pure water. If one assumes that the solute forms an ideal solution in octanol, and that the analyte's solubility is the same in pure water as water saturated with octanol, then the latter two terms in Equation 1 drop out and log(K_{OW}) can be directly correlated with log(S) with an ideal-case slope of -1. The full derivation is given in Appendix A. Numerous coefficients for this QPPR have been published; coefficients from the

following sources were used in this work: EPI Suite's WSKOW program (Meylan and Howard 1996), Chiou et al. (Chiou et al. 1977), Banerjee et al. (Banerjee et al. 1980), and Isnard and Lambert (Isnard and Lambert 1989). Finally, Jain et al. (Jain et al. 2001) presents the General Solubility Equation which begins by defining K_{OW} as the solubility of the analyte in octanol, C_O, divided by the analyte solubility in water, S. By assuming all organic analytes are fully miscible in octanol, a simple correlation between log(S) and log(K_{OW}) is found.

Octanol-water Partition Coefficient

The methods used to estimate log(K_{OW}) were the group contribution of Marrero et al. (Marrero and Gani 2002), the KOWWIN method from EPI Suite (Meylan and Howard 1995), SPARC, and the correlations used above to estimate log(S) from log(K_{OW}).

CHAPTER 3
MATERIALS AND METHODS

Chemicals

Pure samples of each GLV, viz., Methyl Jasmonate (95%), Methyl Salicylate (Reagent plus®, ≥ 99%), 2-methyl-3-buten-2-ol (98%), cis-3-hexen-1-ol (natural, ≥ 98 %) and cis-3-hexenylacetate (≥98%) were obtained from Sigma-Aldrich© and used as received without further purification. Ammonium Nitrate (ACS Reagent, ≥98%), Sodium Hydroxide (Sigma-Aldrich, 99.998%), Sulfuric Acid (BDH, ACS Grade 95-98%) and Ammonium Chloride (ACROS Organics, 99.5%) were used in ionic strength experiments. LC-MS grade water (Honeywell, B&J Brand®) was used to make solutions. Acetonitrile used was from EMD Millipore© (HPLC grade, ≥99.8%).

In order to test the ionic strength effects, ionic solutions were prepared based on the ionic content found in fog waters sampled at Baton Rouge (LA, USA) (Raja et al. 2005): NO_3^- (3 mM), SO_4^{2-} (2 mM), Na^+ (3.3 mM), Cl^- (3 mM), and NH_4^+ (6 mM). Additionally, ionic solutions concentrated by a factor 100 were also used based on the same composition. The ionic solutions have a pH value of 6.

Chemical analysis

All aqueous sample analyses were conducted using HPLC analysis. An Agilent 1100 HPLC-UV/DAD system was used consisting of the following components: a degasser (G1322A), a quaternary pump (G1311A), an autosampler (G1313A), a column compartment (G1316A) and a diode array detector (G1315A). 4 µL of each sample was injected into a 2.1 mm x 150 mm Pinnacle II PAH column (Restek Corp., Bellefonte, PA, USA) with 4µm particle size, held at 40℃. A water:acetonitrile gradient method with a flow-rate of 0.2 $mL \cdot min^{-1}$ was used,

starting with 60% acetonitrile for one minute, ramping linearly to 100% acetonitrile over 6 minutes, followed by a three minute isocratic hold at 100% acetonitrile, and a final ramping down to 60% acetonitrile over 3 minutes, followed by an 8 minute post time at 60% acetonitrile. The UV absorbance of the GLVs was monitored with an average signal at 195 nm for MeJa, MBO, HxO, and HxAC and at 210 nm for MeSa, taking a data point every 2 seconds using the diode array detector with a slit width of 4 nm. The concentration was determined from the measured peak area *via* a calibration curve obtained from the analysis of standard solutions of known concentrations from 0.2-140 $mg \cdot L^{-1}$.

Determination of Henry's Law Constants

Henry's law constants were measured using a modified liquid stripping technique developed in the past for semi-volatile organic compounds (Mackay et al. 1979, Bamford et al. 1999). Figure 4 is a schematic of the equipment used.

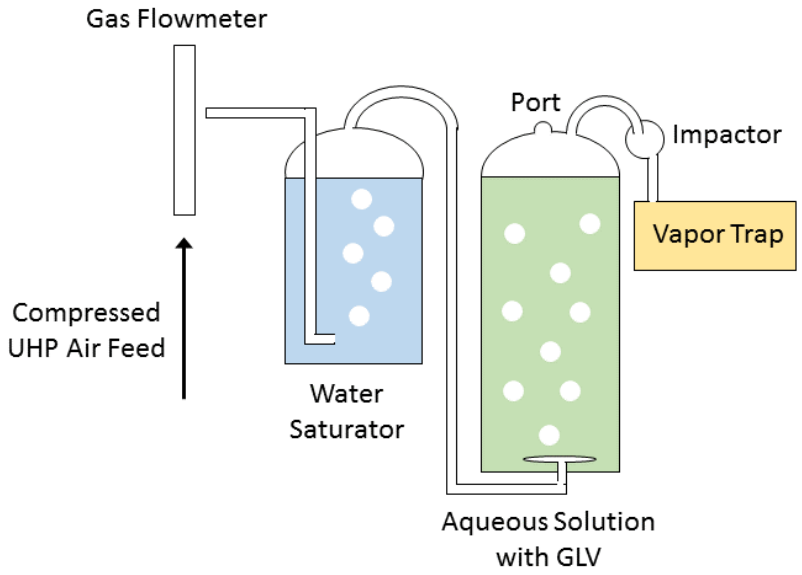

Figure 4. Gas Stripping Apparatus for Measurement of Henry's Constant for GLVs.

Ultra high purity compressed air (Alphagaz 1, Air Liquide©) was passed through a flow-meter (Cole Parmer PMR-1) at 30-45 mL/min before entering a 1 L gas-washing bottle containing LC-MS grade water to saturate the air with water vapor. The air was then bubbled through a coarse

frit at the bottom of a glass bubble column (100 cm length and 5 cm inside diameter) filled with an aqueous solution of GLV to a liquid height of 75 cm. Solutions of GLV were prepared in 3 media: deionized water, ionic solution based on concentration given above, and ionic solution concentrated by a factor 100. The solutions were used in separate Henry's Constant experiments, to determine the effect of ionic strength on the air-water partitioning of each GLVs.

The air bubbles reached equilibrium as they progressed vertically through the column, passed through a glass impactor to remove any solid and liquid aerosols caused by bursting bubbles, and then through an XAD-2 polymeric resin trap (ORBO 43 Supelpak-20, Sigma-Aldrich) to collect airborne GLVs. Each trap has a front and back section; measuring the GLV concentration in these sections separately showed that the maximum GLV found in the back section was less than 5%. For this experiment, both front and back were used. The column was wrapped in a water jacket and insulated to maintain a stable aqueous temperature. The GLVs were desorbed from the XAD-2 trap by soaking in 10 mL of acetonitrile and shaking for two hours. The resulting solution was filtered (PTFE filter, porosity of 0.45 μm, Whatman XD/G) and analyzed by HPLC. Photographs of the top of the column are shown in Figure 5. Sampling intervals ranged from 15 minutes to 24 hours, and at each time point aqueous samples were taken, the temperature was checked, and the sorbent trap was replaced with a new one. The first time point was not included in data analysis because adsorptive effects of the GLV on the top of the apparatus were apparent, and the determined K_H was higher than all of the others. The ratio of the average aqueous concentration (C_W) to the measured air concentration (C_A) was used to obtain the Henry's Law constant, K_H [$M \cdot atm^{-1}$].

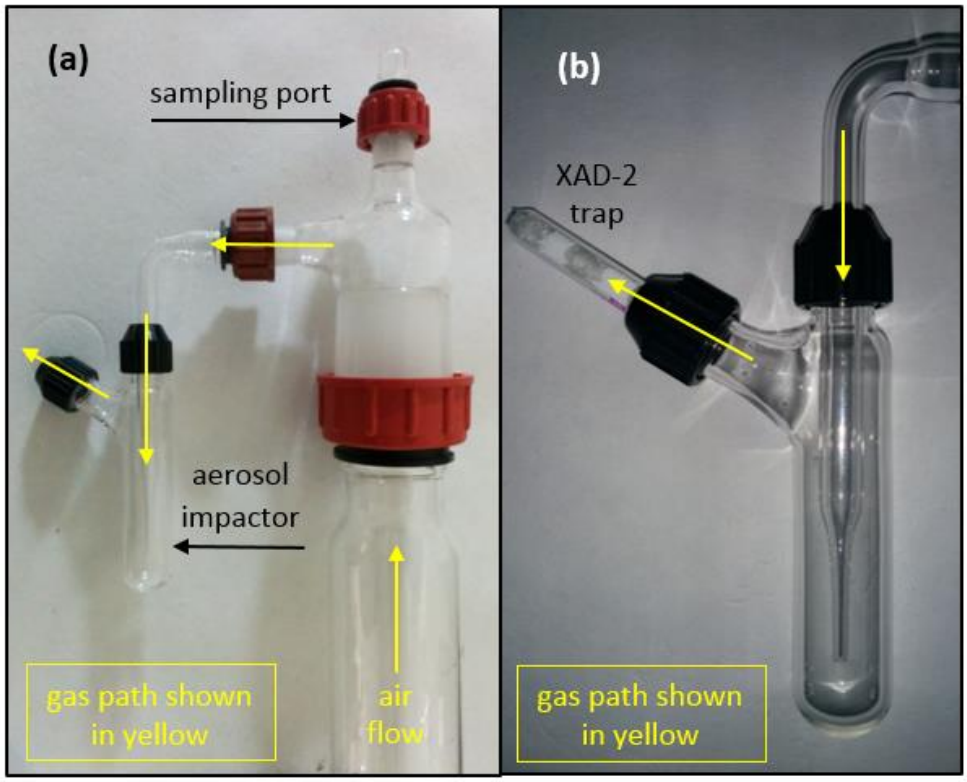

Figure 5. (a) The top of the column, not including XAD-2 trap (b) close-up view of aerosol impactor and XAD-2 resin gas trap.

Determination of Saturation Aqueous Solubility

Aqueous solubility S [mM] was measured using a traditional batch equilibration shake flask technique (Banerjee et al. 1980). Ten 40 mL amber borosilicate vials with PTFE lined caps (VWR 93001-538) were each filled with 35 mL LC-MS grade water. GLV was added to each vial in increasing amounts, with the highest mass added corresponding to double the solubility estimated by the WATERNT program from EPI Suite (EPA 2012). The sealed vials were allowed to equilibrate over several days while gently shaken in a water bath at 25°C. After the equilibration period, the shaker was turned off, and the samples kept in the bath for 24 hours, to allow un-dissolved solute to settle to the bottom or rise to the top. Aliquots of 2 mL were taken from the middle of the liquid volume and centrifuged at 12,000 rpm for 15 minutes. Aqueous samples were then taken from the aliquots and diluted for analysis with HPLC. As the solubility

limit was approached and passed, the aqueous concentration plateaued. The solubility limit was determined as the average of these plateau increased GLV concentrations until the plateau was apparent.

CHAPTER 4
RESULTS AND DISCUSSION

Henry's Law Constants at 25°C

Henry's law is the relationship between the equilibrium concentrations of a compound in the aqueous and air phases. The air stripping technique used requires that the method be first validated using a compound of known Henry's constant. In this case we chose an aromatic compound, viz., benzene. Using the instrumentation described in this work, the measured K_H of benzene is 0.19 ± 0.03 $M \cdot atm^{-1}$ which compares well with literature values of 0.19 – 0.21 $M \cdot atm^{-1}$ (Mackay et al. 1979, Ashworth et al. 1988, Dewulf et al. 1995, Karl et al. 2003). Measurements of the gas phase and aqueous phase concentrations were made at regular intervals and the ratio of gas to aqueous phase concentration are plotted as shown in Figure 6 for a typical run for MeSa.

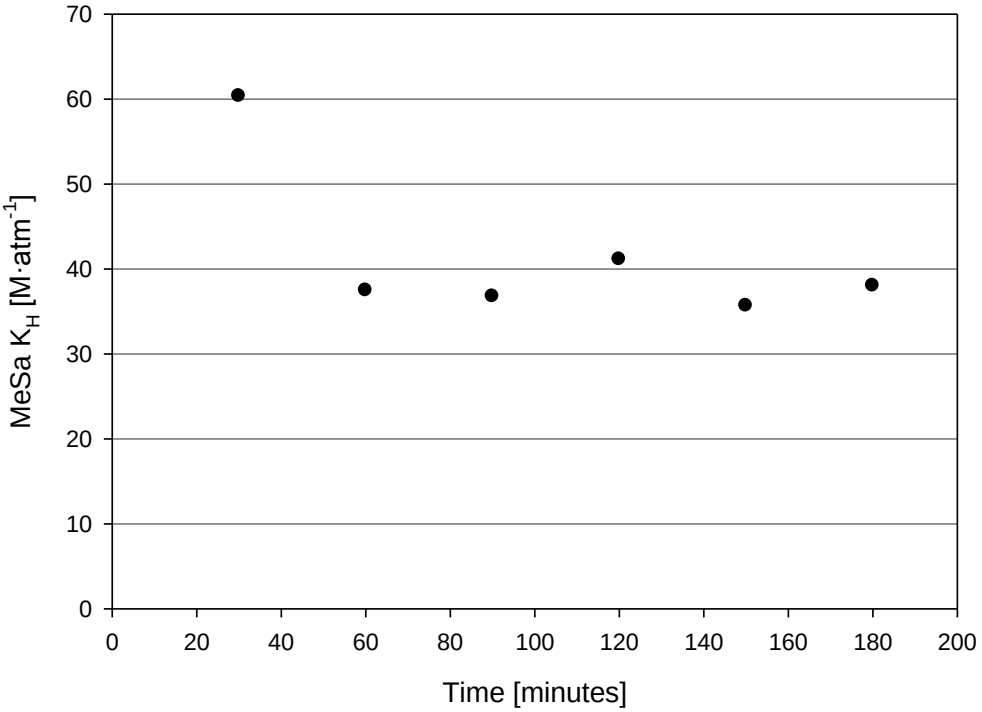

Figure 6. MeSa K_H vs Time at 25°C showing asymptotic values.

It is clear that the values tend to be large initially and then reaches an asymptote; this value is taken to be the equilibrium ratio. The measured Henry's law constants for the five GLVs at 25, 30 and 35°C are displayed in Table 2.

Table 2. Values of K_H [$M \cdot atm^{-1}$][a] for GLVs with at various temperatures.

GLV	25°C	30°C	35°C	Literature Values (25°C)
MeJa	8091 ± 1121	6716 ± 1272	4837 ± 272	5018[b]
MeSa	37.9 ± 2.1	16.4 ± 0.9	10.0 ± 4.2	33.5[b]
MBO	52.9 ± 5.1	40.2 ± 5.4	31.7 ± 2.2	48[c]
HxO	113 ± 7.1	83.4 ± 8.3	62.7 ± 3.0	Not Available
HxAC	3.6 ± 0.2	3.2 ± 0.2	2.7 ± 0.2	3.3[d]

[a]Values given ±1 Standard Deviation. [b](Karl et al. 2008). [c]Altschuh, Brüggemann et al. 1999). [d](Karl et al. 2003)

The existing values of K_H for these GLVs found in the literature are also given Table 1, but most are available only at 25°C. Between the measured values and those obtained from the literature, there is agreement only for three of the five compounds, viz., MeSa, MBO and HxAC. For MeJa there is considerable disagreement with the literature values. The highest Henry's constant is that for MeJa and the lowest is for HxAC. As K_H increases, the partitioning of compounds is biased towards the aqueous phase. Thus, the chemistry for MeJa in atmospheric systems is going to be determined primarily by the aqueous phase processes. The breakpoint for such behavior is typically $K_H > 1000\ M \cdot atm^{-1}$ (Gelencser 2005). Hence for all other GLVs the aqueous phase processes are less important.

As mentioned in Chapter 2, in addition to the measured values six quantitative structure-property relationships (QSPRs) were used to predict the K_H values. GLVs present a challenge for property estimation because all the GLVs have multiple functional groups producing a complex polar character whose hydrogen bonding interactions can be difficult to capture. This is reflected in Figure 7 which compares the experimentally determined K_H for each GLV with the estimated values from the above methods.

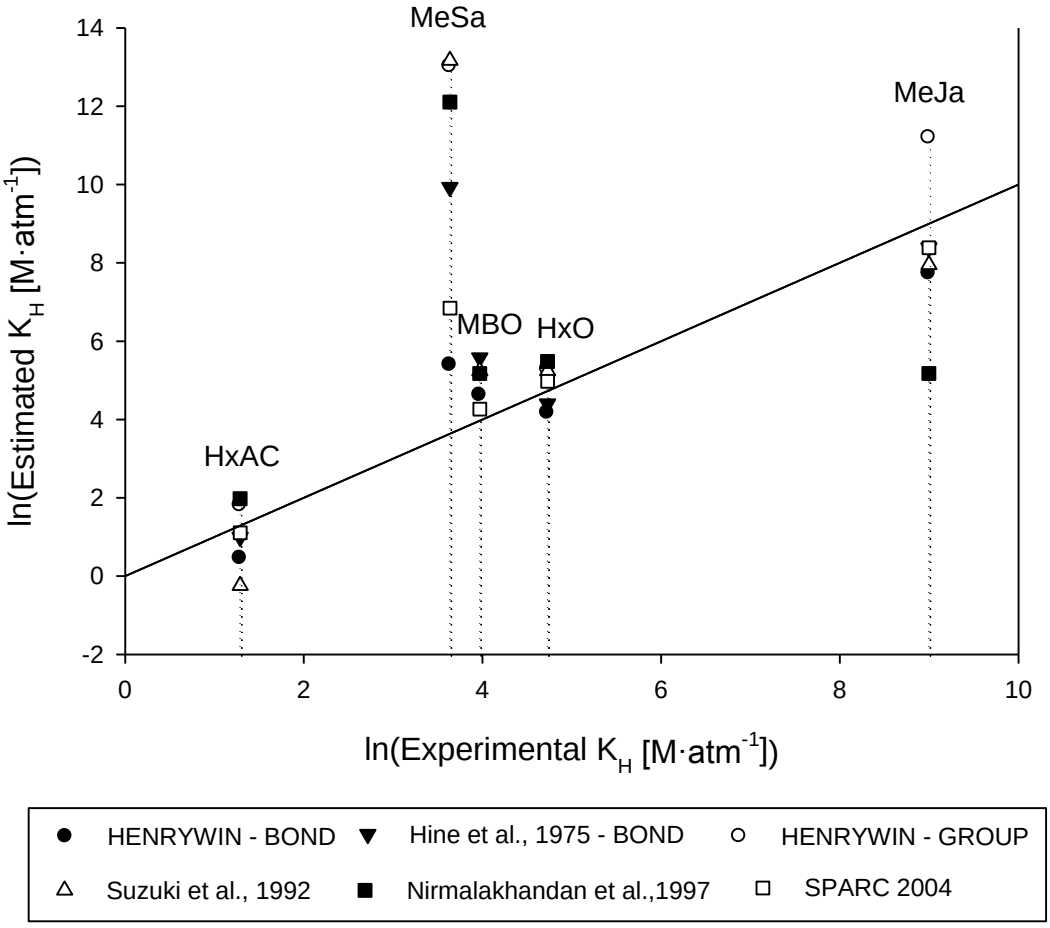

Figure 7. Comparison of experimentally determined K_H at 25°C with estimated values.

The estimation methods performed satisfactorily for the three lower molecular weight compounds with relatively simple functional group combinations: HxO, HxAC, and MBO, but not for MeSa and MeJa. The range of estimation values for HxO (64.5 M·atm^{-1} to 196 M·atm^{-1}) contained the measured value, with the most accurate being the bond method of Hine & Mookerjee (1975) (81. 7 M·atm^{-1}). For HxAC, the estimations were again all accurate, the range (0.78 M·atm^{-1} to 7.23 M·atm^{-1}) contained the measured value and all estimations were within one order of magnitude, with the best performing being SPARC (3.02 M·atm^{-1}). For MBO, all of the estimations (70.8 M·atm^{-1} to 264 M·atm^{-1}) including the best performing (SPARC, 70.8 M·atm^{-1}) produced values higher than the measured value, showing a consistent overestimation

of the molecule's distribution towards the aqueous phase. However, the estimation methods were inadequate for predicting K_H of MeJa and MeSa, with the ranges of estimations spread over many orders of magnitude. For MeJa, the range (177 $M \cdot atm^{-1}$ to 72,464 $M \cdot atm^{-1}$) was very large, but was affected by the excessively high and low values respectively given by HENRYWIN – GROUP and Nirmalakhandan et al. (1997) respectively. The best performing was again that of Hine et al. (1975). The estimations for MeSa were even more scattered, the range of estimations (216 $M \cdot atm^{-1}$ to 195,588 $M \cdot atm^{-1}$) spanned many order of magnitude and didn't even include the measured value. Here there were no outliers skewing the range, and even the best performing HENRYWIN – BOND method value was almost 10 times the measured value. For both MeJa and MeSa, the multiple functional groups clearly affected the predictive ability of the methods. For MeSa, especially, all methods appeared to have greatly overestimated the hydrogen bonding that the hydroxyl and ester groups would lend, while neglecting the nonpolar character of the aromatic ring. Overall, however, most correctly identified MeJa as having the largest K_H and HxAC as the smallest. The overall best performing estimators (judged by sum of squared relative errors) were HENRYWIN – BOND program, followed closely by the SPARC program. This is an interesting result given that group contribution methods are thought to be more accurate than bond contribution methods (Staudinger and Roberts 1996). Here, the HENRYWIN – BOND method was not only more applicable (HENRYWIN – GROUP returned an incomplete fragment value when estimating K_H for MBO) but also more accurate than the HENRYWIN – GROUP method, even when omitting MeSa and MeJa from consideration.

Henry's Law Constants at varying temperature

The variation of the Henry's constants with temperature is an important parameter in the assessment of the atmospheric aqueous chemistry. The variation can be expressed using Equation 2 (Valsaraj 2009).

$$\ln K_H = A - \frac{B}{T} \quad (2)$$

A and B are constants and T is temperature [K]. From the constants A and B, the enthalpy of phase change from liquid to gas ΔH [kJ·mol^{-1}] and the entropy of phase change ΔS [kJ·mol^{-1}·K^{-1}] for each compound can be found (Bamford et al. 1999). The results are shown in Table 3.

Table 3. Measured enthalpy and entropy of phase change each GLV from T varied K_H.

GLV	A	B	ΔH (kJ·mol^{-1})[a]	ΔS (J·mol^{-1}·K^{-1})[b]	r^2
MeJa	-0.1015	4719.5	36.7 ± 13.2	21.6 ± 21.8	0.969
MeSa	30.50	12221	99.1 ± 28.3	276 ± 47	0.980
MBO	4.913	4706.2	36.6 ± 2.5	63.2 ± 4.2	0.999
HxO	6.518	5412.1	42.5 ± 0.8	76.6 ± 1.3	0.999
HxAC	2.278	3126.3	23.5 ± 10.3	41.3 ± 17.3	0.954

[a]Values given ±2 Standard Errors of the slope. [b]Values given ±1 Standard Errors of the intercept

The ΔH values ranged from (23.5 ± 10.3) kJ·mol^{-1} to (99.1 ± 28.3) kJ·mol^{-1} for HxAC and MeSa respectively. These are consistent with the ΔH of non-aromatic, oxygenated alkenes (Chickos and Acree 2003). For MBO, HxO, and HxAC they are similar to enthalpy of vaporization for unsaturated counterparts: 50.3 kJ·mol^{-1} for 2-methyl-2-butanol, 61.1 kJ·mol^{-1} for 1-hexanol, and 52.1 kJ·mol^{-1} for hexyl acetate (Chickos and Acree 2003). Double bonds have been shown to decrease the enthalpy of vaporization but generally only by 1-2 kJ·mol^{-1} for alkanes (Baev 2012). The rest of the discrepancy may be attributed to the fact that the cited values of enthalpy of vaporization are calculated as the energy required to vaporize the pure compound from its pure liquid, however the enthalpy required to vaporize the GLV from an aqueous solution may be higher due to hydrogen bonding. The ΔH of MeSa compares favorably with that of other oxygenated aromatics such as benzoic acid (89.5 ± 0.16) kJ·mol^{-1} (Morawetz

1972). The ΔS values ranged from (22 ± 21) $J \cdot mol^{-1} \cdot K^{-1}$ (MeJa) to (276 ± 47) $J \cdot mol^{-1} \cdot K^{-1}$ (MeSa). MeJa, HxO, MeSa, and HxAC have values within the expected range for organic compounds, while MeSa's high value compares well with that of benzoic acid (261 $J \cdot mol^{-1} \cdot K^{-1}$) (Torres-Gómez et al. 1988).

Henry's Law Constants at varying ionic concentrations

In the literature it has been reported that K_H for glyoxal increases by as much as 50 times in the presence of sodium sulfate (Ip et al. 2009). Hence, the extent to which partitioning behavior of GLVs would be affected by environmentally relevant fog water composition was determined by performing an experiment at ionic strength comparable to actual fog water. One solution had an ionic composition similar to the fog water (0.01 M) and the other one had a composition 100 times (1 M) comparable to that of an industrial wastewater. The K_H obtained in the two solutions and in ultrapure water are displayed in Table 4.

Table 4. K_H [M/atm][a] of GLVs at varying ionic concentrations at 25°C

GLV	LC-MS grade water	Ionic solution (1x)	Ionic solution (100x)
MeJa	8091 ± 1121	5454 ± 520	3869 ± 261
MeSa	37.9 ± 2.1	26.7 ± 3.4	20.1 ± 1.6
MBO	52.9 ± 5.1	38.7 ± 2.2	21.8 ± 4.4
HxO	113 ± 15	140 ± 18	132 ± 11
HxAC	3.6 ± 0.2	3.3 ± 1.1	2.3 ± 0.2

[a]Values given ±1 Standard Deviation

The magnitude of these values relative to the value in LC-MS grade water is given in Figure 8.

For MeJa, MeSa, MBO, and HxAC the K_H value is clearly affected by the ionic strength of the liquid phase. HxO is the only GLV that appears unaffected. These results are in general agreement with previous findings that ionic species introduce a "salting-out" effect which reduces a compound's aqueous solubility and shifts its air-water partitioning behavior towards the gas phase. The higher molecular weight GLVs with carbonyl groups all show this effect. However, 1-alkanols have previously been shown to have a decreased salting out effect from

sodium sulfate than 2-ketones due to the ability of the alcohol group to hydrogen bond with water more than the carbonyl (Falabella et al. 2006). The fact that MBO undergoes salting out can be attributed to steric hindrance to water accessing its hydroxyl group.

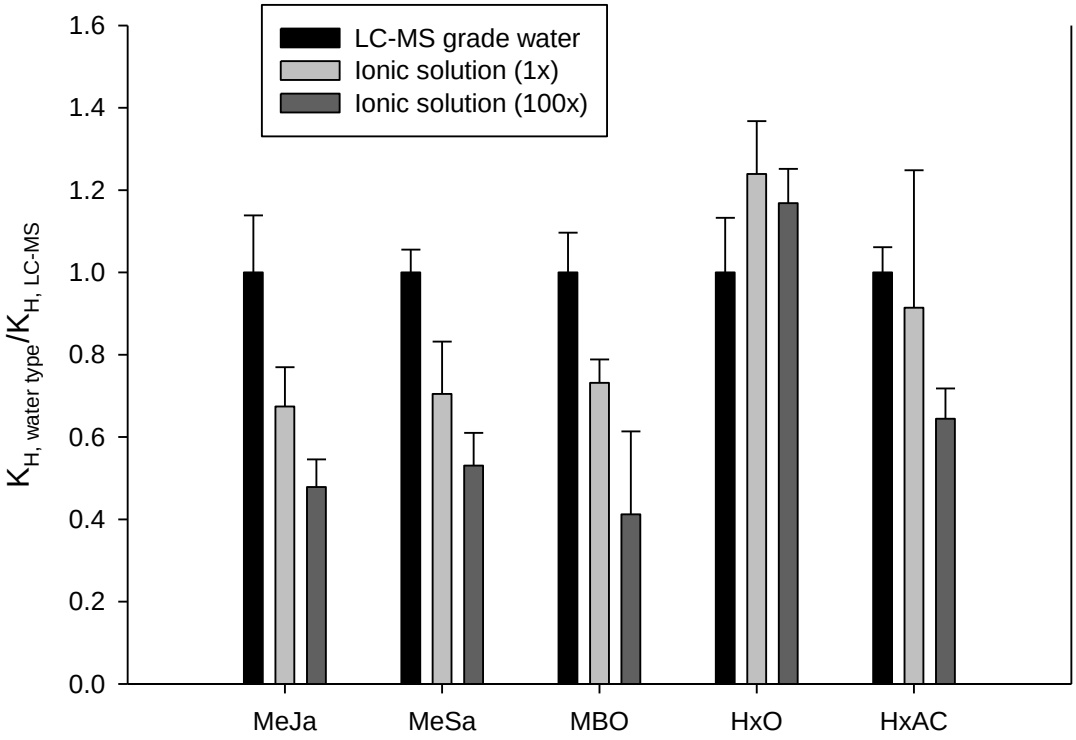

Figure 8. K_H [$M \cdot atm^{-1}$] of GLVs at varying ionic concentrations at 25 °C, error bars represent 1 standard deviation.

Aqueous Solubility

The measured aqueous solubility of GLVs are presented in Table 5.

Table 5. Measured Aqueous Solubility and log(K_{OW}) of GLVs.

GLV	Solubility [mM]	log(K_{OW})
MeJa	4.52 ± 0.09	2.55 ± 0.02
MeSa	5.11 ± 0.06	2.36 ± 0.02[a]
MBO	1959 ± 36	0.69 ± 0.02[b]
HxO	162 ± 6	1.52 ± 0.02[c]
HxAC	3.12 ± 0.17	2.48 ± 0.02[c]

[a] (Liyana-Arachchi et al. 2013). [b] (Liyana-Arachchi et al. 2013)[c] (Liyana-Arachchi et al. 2014)

The solubility of MBO (1959 ± 36 mM) clearly dwarf that of the other GLVs, unsurprising because it is the lightest molecular weight GLV and its hydroxyl group lends significant hydrogen bonding opportunity. The solubility of HxO (162 ± 6 mM) was also relatively large because of the hydroxyl group bonded to the first carbon, but less than MBO because of its extra carbon atom and straight-chain enol structure which exposes more non-polar surface area to interact with water. The other three GLVs exhibited modest aqueous solubility, as both MeJa (4.52 ± 0.09 mM) and HxAC (3.12 ± 0.17 mM) were under 5 mM while MeSa was just over (5.11 ± 0.06 mM). Neither HxAC nor MeJa has any alcohol groups, but ester groups lend enough polar character to solubilize appreciably. The straight chain structure of HxAC clearly limits its solubility, and it is interesting to note the difference in solubility between HxAC and HxO by simply replacing HxAC's ester group with a hydroxyl group. MeSa's aromatic ring dampened the influence of the aromatic alcohol and ester group – the increased bulk also contributed to its low solubility. However even though the differences in solubility are large, even the least soluble GLV should not be expected to reach its aqueous saturation value in environmental conditions.

In all, eight different estimations for solubility were used: two based only on molecular structure, the other six were correlations using previously determined experimental values of $\log(K_{OW})$ to estimate S, as mentioned in Chapter 2. These estimated values are plotted against the experimental values in Figure 9. For MeJa, both the group and bond contribution schemes under predicted the solubility, presumably due to difficulty to decipher the effect of the many multifunctional groups. The correlations all predicted it very well, with the best performing being Chiou et al. (1977) (4.54 mM compared to 4.52 ± 0.09 mM). MeSa again proved to be difficult for group contribution schemes to predict, with both group and bond methods overestimating the solubility, again over-predicting the extent of hydrogen bonding due to the

aromatic hydroxyl and ester groups. The correlations were much closer, but still over predicted slightly, with the best method again being the correlation of Chiou et al. (1977) (8.72 mM compared to 5.11 ± 0.06 mM

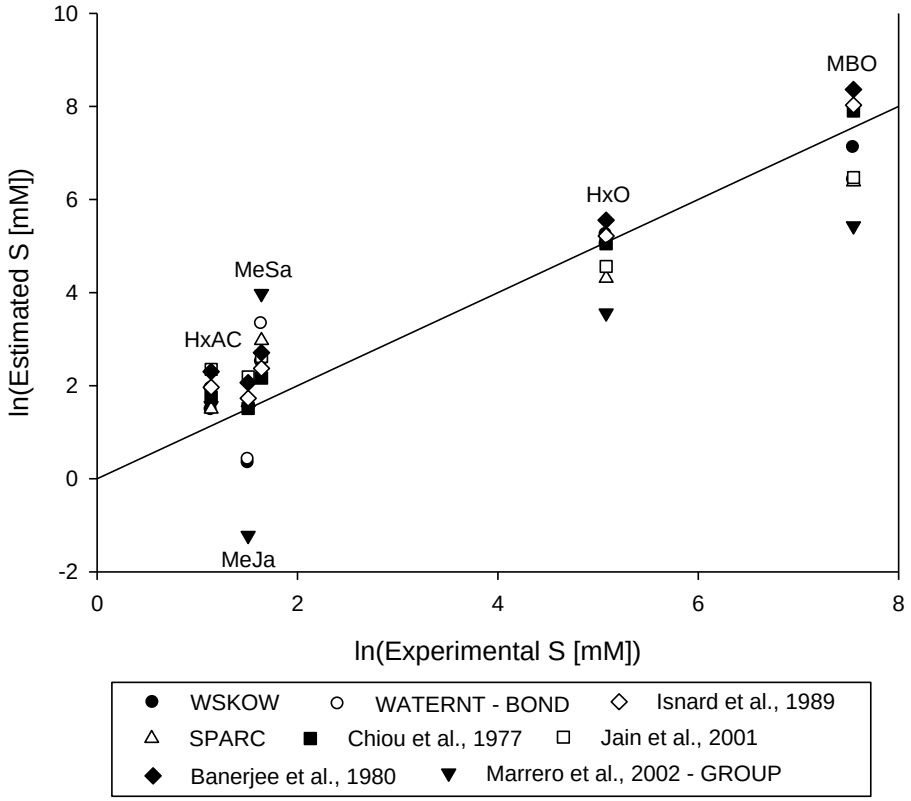

Figure 9. Comparison of Experimental and Predicted Aqueous Solubility of GLVs.

The range of predictions for MBO (228 mM to 4289 mM) was very large, and erred by deviating both positively and negatively from the measured value. Both group contribution methods under-predicted, and the closest correlation value was from EPI Suite's WSKOW program, some 65% of the measured value (1230 mM compared to 1959 ± 36 mM). For HxO however, the methods showed better accuracy, especially the WATERNT method. The best was again that of Chiou et al. (1977) (156 mM compared to 162 ± 6 mM), but all methods except the group method of Marrero et al. (2002) provided acceptable estimations. For HxAC, all methods provided very good estimations, including both group contribution methods and SPARC, however all slightly

overestimated the value. The closest came from WSKOW (4.39 mM compared to 3.12 ± 0.17 mM).

The two best performing estimations were those of Chiou et al. (1977) and EPI Suite's WSKOW program, both from measured log(K_{OW}) values. Either the correlation of Chiou et al. (1977) or WSKOW program had the best solubility estimation for every GLV. Overall, all methods generally identified MBO as the most soluble, HxO as less soluble than MBO, and MeSa, MeJa, and HxAC as far less. As in the prediction of Henry's Constants, the group contribution method appeared to struggle with both MeJa and MeSa, the two most complex GLVs. This highlights a severe limitation with EPI Suite: its consistent inability to estimate the properties multifunctional compounds like GLVs. EPI Suite is widely used in environmental calculations but it's clear that its estimations should be used with great caution. Since group contribution methods predict properties "from scratch", it is somewhat unfair to compare them to the correlations based on accurate experimental values. Neither the Chiou et al. (1977) nor WSKOW correlations used the ideal-case slope of -1 for the relation between log(K_{OW}) and log(S), yet were more accurate in this case than the other correlations which were closer to ideality. Though in the idealized case the slope should be -1, others have found (Isnard and Lambert 1989) that over a large training set this does not bear true. This discrepancy has been attributed to non-ideal behavior resulting from the mutual saturation of water and octanol (Chiou et al. 1982). This can be explained by examining Equation 1: while octanol is only slightly soluble in water, water is highly soluble (2.3 M (Chiou et al. 1982)) in octanol which directly affects molar volume $\bar{V}_0^*$ and could affect the γ_O term, depending on the analyte. Past papers have found that grouping monofunctional compounds by class increases correlational accuracy and pushes the slope toward unity (Tewari et al. 1982). However, for multifunctional compounds

like GLVs, using a general correlation trained on a varied dataset of compounds with a wide variety of functional groups appears to be the best choice. This may be because of non-ideal conditions as specified above affecting the process. When estimating the aqueous solubility of multifunctional compounds such as GLVs, a correlation with an experimentally determined log(K_{OW}) is preferable to group contribution methods, as noted elsewhere (Meylan and Howard 1996).

1-Octanol/Water Partition Coefficient

In previous works from our laboratory, the log(K_{OW}) values for MBO, HxO, HxAC, and MeSa were measured (Liyana-Arachchi et al. 2013, Liyana-Arachchi et al. 2013, Liyana-Arachchi et al. 2014). They are presented in Table 5 along with the measured value for MeJa. The log(K_{OW}) values reflected the solubility trends: the most soluble GLV (MBO) partitions strongly to the aqueous phase, followed by the second most soluble (HxO), followed distantly by MeJa, MeSa, and HxAC. These values are plotted in Figure 10 against the estimated values mentioned in Chapter 2.

Here again, the Chiou et al. (1997) correlation is clearly the most accurate. This is unsurprising, given that the KOWWIN and WATERNT estimations are both based on the same bond/fragment contribution methodology (Meylan and Howard 1991), and the other correlations fared worse than Chiou et al. (1977) in predicting log(S) from log(K_{OW}). The correlation from Chiou et al. (1977) was the most accurate for every GLV except HxAC. Unlike for aqueous solubility, however, the fragment contribution method from Meylan et al. (1995) (in the form of KOWWIN) produced acceptable results.

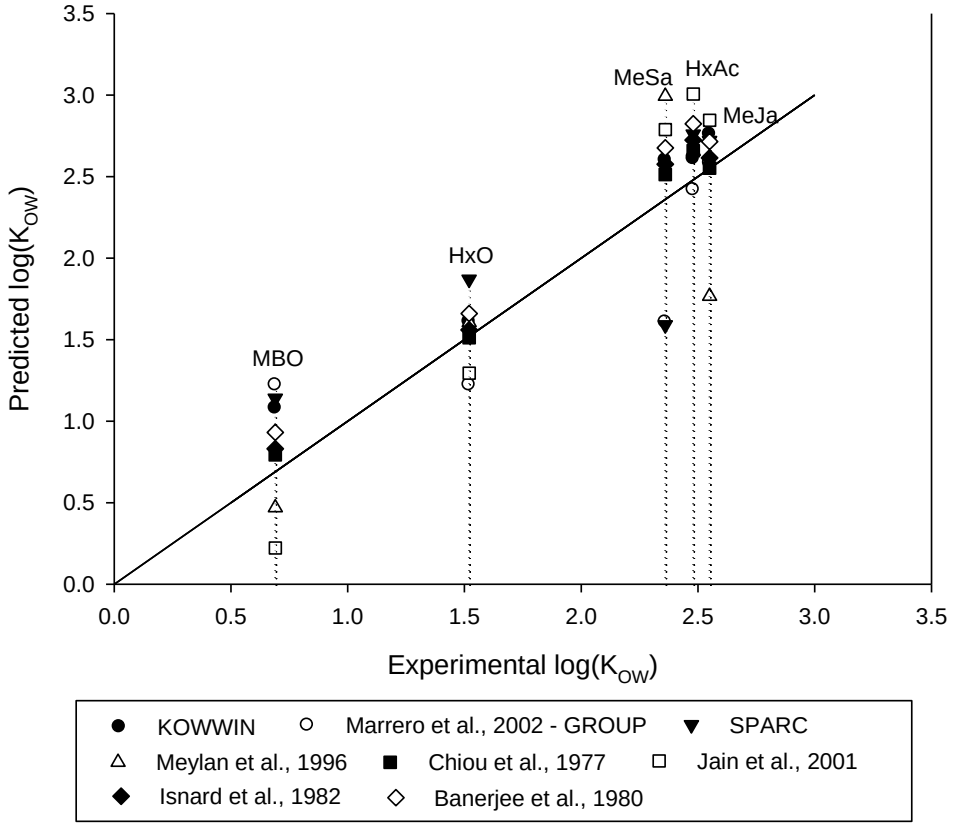

Figure 10. Comparison of Experimental and Predicted octanol/water partition coefficients of GLVs

It is again shown that the correlation from Chiou et al. (1977), containing a non-unity slope is the most accurate predictor of log(K_{OW}). It has previously been shown that alkanes and alkenes deviate consistently downwards from the ideal line (Chiou et al. 1982), caused by a large γ'_O term which indicates significant analyte interactions with the octanol phase. It is not anticipated that the small amount of octanol dissolved in water would cause such large deviations from ideality in the aqueous phase $\frac{\gamma'_W}{\gamma_W}$ term for compounds already fairly soluble in water.

For multifunctional compounds such as GLVs, measuring either log(K_{OW}) or S will aid significantly in predicting the other. If no values are available, caution should be taken in

estimating the solubility from group or fragment contribution methods, especially if the compound of interest is an aromatic with polar functional groups.

Implications for Secondary Organic Aerosol Production in Fog Droplets

In order to consider the impact GLVs will have on aqueous phase SOA production, it is necessary to examine not only their reactions in the bulk aqueous phase, but also their heterogeneous reactions with gas-phase oxidants while adsorbed at the air-water interface. This "interface phase" can be a significant site for oxidation of VOCs in aqueous droplets with large surface area to volume ratios such as fog and clouds (Wadia et al. 2000, Mmereki and Donaldson 2003, Liyana-Arachchi et al. 2013). The amount of analyte residing in the surface phase of a droplet is represented by the surface concentration C_S [mol·m^2]. In previous works the surface tension of droplets of aqueous solutions with GLVs was measured at varying bulk aqueous concentrations of GLVs C_W (Liyana-Arachchi et al. 2014). Using Equation 3, the change in surface tension can be related to the change of natural logarithm of the bulk aqueous concentration C_W to find a surface concentration C_S.

$$C_S = -\frac{d\sigma}{d\mu_{GLV}} = -\frac{1}{RT}\frac{d\sigma}{d\ln(C_W)} \qquad \text{Equation 3}$$

Here C_S is the surface concentration, σ is the surface tension, μ is the chemical potential of the GLV, R is the gas constant, and T is the temperature. By taking the ratio of the surface concentration C_S to its corresponding bulk concentration C_W at equilibrium, a surface to bulk aqueous partition coefficient K_{SW} [m] was calculated, giving an indication of the extent to which a compound partitions to the air-water interface of an aqueous body vs the bulk. Furthermore, an air-surface partition coefficient K_{SA} [m], as defined previously was obtained by multiplying K_H with K_{SW}. These values are given for the GLVs in Table 6 below.

Table 6. K_{SW}, K_H, and K_{SA} for all GLVs at 25°C.

GLV	$K_{SW} \cdot 10^{-4}$ [m][a]	K_H [M/atm][a]	$K_{SA} \cdot 10^{-4}$ [m]
MeJa	13.4 ± 0.87	8091 ± 1121	2648
MeSa	3.87 ± 1.76	37.9 ± 1.7	3.59
MBO	1.71 ± 1.53	52.9 ± 5.1	0.050
HxO	4.28 ± 2.95	113 ± 15	16.7
HxAC	25.4 ± 15.7	3.6 ± 0.2	2.24

[a] Values given ± 1 Standard Deviation

HxAC has the highest K_{SW}, followed by MeJa. These relatively hydrophobic compounds intuitively will leave the bulk aqueous and head towards the surface, where interactions with polar solvent water are decreased. The two most soluble compounds, MBO and HxO have very low K_{SW} as well, indicating their comfort with the bulk aqueous phase. Interestingly MeSa has a very low K_{SW}, so while it is relatively hydrophobic and does not dissolve well in water, this does not translate into a preference for the air-water interface. With these three coefficients, in an air-water system containing GLV at equilibrium, if either bulk aqueous, surface aqueous, or gas phase concentration is known, the two other parameters can be calculated.

By assuming a GLV mixing ratio in the atmosphere of 500 ppt (Jardine et al. 2010), it is possible to determine the bulk and surface aqueous concentrations for an aqueous body in equilibrium with this atmospheric composition. The calculated values of surface and bulk aqueous concentrations for water in equilibrium with a GLV gas phase are displayed Table 7.

Table 7. Surface and bulk aqueous concentrations for water in equilibrium with gas phase GLV.

GLV	Surface Aqueous Concentration $\cdot 10^{-5}$ [μmol·m^{-2}]	Bulk Aqueous Concentration $\cdot 10^{-2}$ [μM]
MeJa	543	405
MeSa	0.736	1.90
MBO	0.011	2.65
HxO	2.43	5.66
HxAC	0.459	0.18

Due to its large K_H, MeJa has the largest concentration in both bulk and surface aqueous phases. This has significant implications in fog where the high MeJa concentrations will render it the

primary SOA source compared to the other GLVs studied here. The bimolecular rate constants of the five GLVs in the presence of hydroxyl radicals have been determined by competition kinetics and indicate that while MeJa has a low rate constant relative to the other GLVs, (Richards-Henderson et al. 2014) its relatively massive equilibrium aqueous phase concentration leads to faster reaction rates.

This is illustrated by considering the example of an ensemble of fog droplets in a finite volume of air, and a GLV in equilibrium between the two. Since fog sized aqueous droplets have high surface area to volume ratios, air-water interfacial adsorption must be accounted for, so the GLV is in equilibrium between three phases: bulk aqueous, surface aqueous, and gas. By assuming the liquid water content, L, in the finite volume is that of dense fog (1 [g water·m^{-3} total] (Seinfeld and Pandis 1998)), and that this water exists only as spherical droplets, the fraction of total GLV in the volume partitioned into the bulk and surface aqueous phases, called the droplet scavenging efficiency, can be calculated as a function of droplet diameters (Valsaraj 2004).

$$\varepsilon = \frac{n_W + n_S}{n_O} = \left(1 + \frac{1}{LRTK_H\zeta}\right)^{-1} \quad \text{Equation 4}$$

Here ε is the droplet scavenging efficiency, n_W and n_S are the number of moles of analyte in the bulk and surface aqueous phases respectively, n_O is the total number of moles in the ensemble (equal to the sum of n_W, n_S and the number of mols in the gas phase), L is the liquid water content, R is the gas constant, T is temperature, and ζ is the deviation from conventional Henry's Constant relationship for bubbles in water, defined in Equation 5 below.

$$\zeta = 1 + \frac{6}{d}(K_{SA}/(RTK_H)) \quad \text{Equation 5}$$

Here d is the droplet's diameter. ζ in practice denotes the enhancement in uptake if the surface phase is significant, and approaches 1 as the surface-to-air partition constant, K_{SA} approaches 0.

The droplet scavenging efficiency is calculated for each GLV and the results are shown in Figure 12 below.

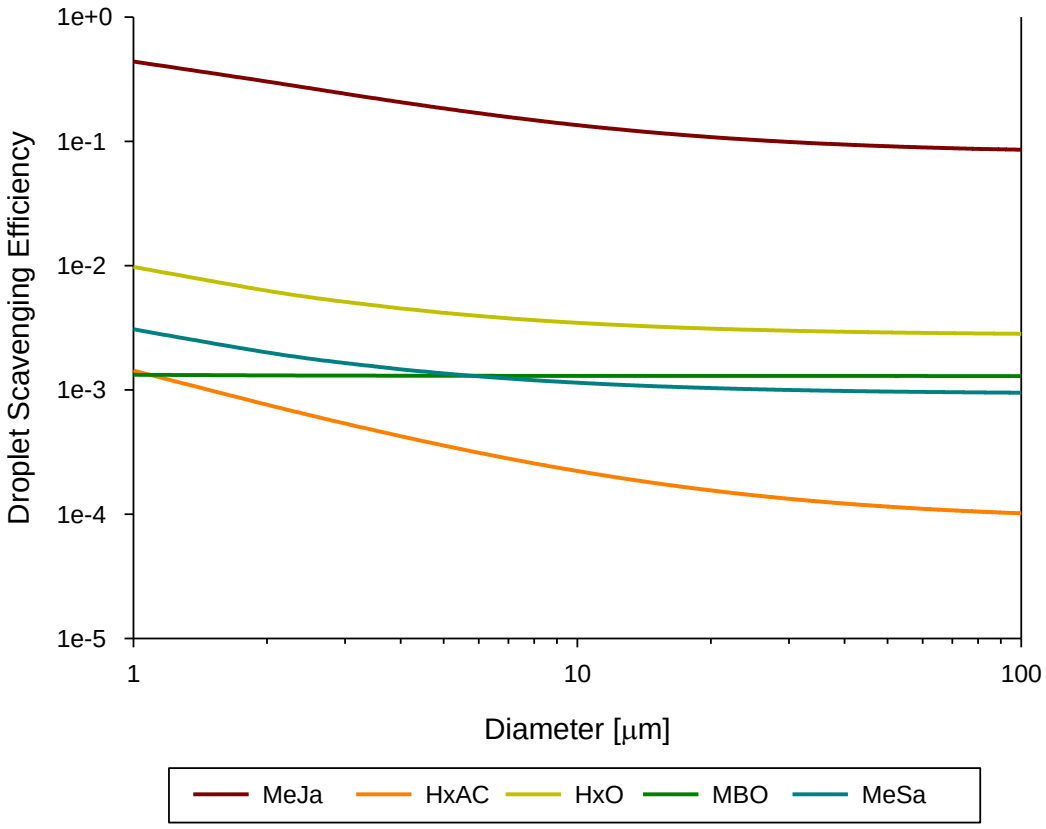

Figure 12. Droplet Scavenging Efficiency for GLVs at 25°C.

Many insights relevant to SOA production can be gleaned from this plot. First, by comparing the scavenging efficiencies of the five GLVs at d = 100 μm (where ζ will be closest to one), it is found that ε decreases according to decreasing K_H of the GLV. For large aqueous droplets of 100 μm, the surface area to volume ratio is low and bulk dissolution is more significant than surface adsorption, so it is intuitive that that Henry's Constant will be the main determinant of ε. Hence, MeJa and HxAC have the highest and lowest ε respectively, and have the highest and lowest K_H as well. Then, by tracing the ε curves towards smaller droplet diameters, we see ε increases with decreasing droplet diameters. This is because ζ increases as droplet diameter decreases, which in turn increases the scavenging efficiency ε. This again

makes logical sense: for the same aqueous volume, increasing the surface area available for adsorption (by way of smaller droplet diameters) will result in more GLV being adsorbed to the air-water interface at equilibrium. The difference between ε at diameter of 1 and 100 μm is determined by the magnitude of the K_{SW} term. For HxAC, the GLV with the largest K_{SW}, this difference is large, but for MBO, the GLV with the smallest K_{SW}, the difference is minimal.

Overall, the plot clearly indicates the importance of MeJa in aqueous phase processing. At droplet diameters of 1 μm, almost half of MeJa can be found in the surface or bulk aqueous phases. Even at droplet diameter 50 μm where the surface phase is a negligible store for MeJa, almost 7% of the total MeJa molecules reside in the droplet. For most of the other GLVs, the air-water interface is a significant store, especially at small droplet sizes. Only MBO does not show a significant variation due to droplet size, due to its low K_{SW}.

This example can be used to elucidate the partitioning behavior of GLV molecules between surface and bulk phases in the aqueous droplet alone. Consider only the mols on the surface n_S and the mols in the bulk n_W. The ratio of n_S to n_W can be easily found by manipulating the K_{SW} definition as in Equation 6 below.

$$\frac{n_S}{n_W} = \frac{C_S * Droplet\ Surface\ Area}{C_W * Droplet\ Volume} = K_{SW} * \frac{3}{r} \qquad \text{Equation 6}$$

Here r is the droplet radius. This gives the ratio of the number of mols on the droplet surface to the number of mols in the droplet's bulk, which is then used to find the percentage of the individual droplet's total mols (n_S + n_W) which can be found on the droplet's surface. A plot showing this percentage of the total number of mols in each aqueous droplet which reside on the droplet's surface as a function of droplet radius is shown Figure 13 below. For example, in the case of HxAC, the molecule with the largest K_{SW}, up to 80% of the GLV molecules are on the surface for a water droplet of 2 μm radius. MBO, with the lowest K_{SW}, has almost no GLV

residing in its surface phase. The calculation emphasizes that not only is the aqueous phase significant for GLV scavenging, but that for fog-sized aqueous droplets, the air-water interface can be a significant store for GLVs compared to the bulk phase.

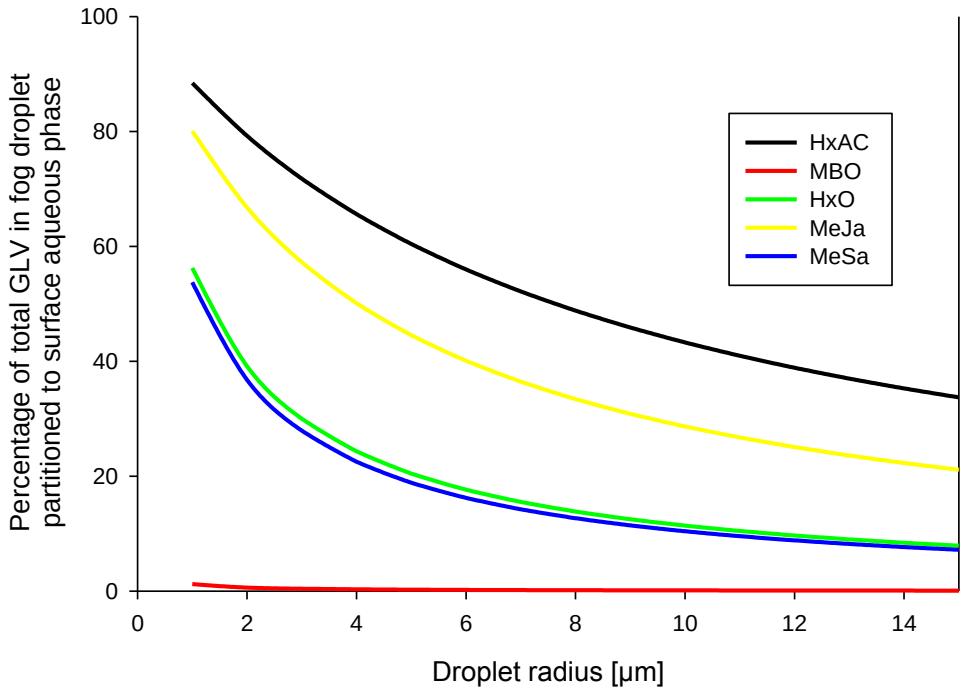

Figure 13. The percentage of GLV in the aqueous phase of a theoretical fog droplet which is adsorbed to the air-water interface

CHAPTER 5
CONCLUSION

In this study, various physical properties of a class of biogenic volatile organic compounds called green leaf volatiles have been determined. Experimental values of the Henry's Constant, aqueous solubility, and 1-octanol/water partition coefficient of five GLVs (Methyl Jasmonate (MeJa), Methyl Salicylate (MeSa), 2-methyl-3-buten-2-ol (MBO), cis-3-hexen-1-ol (HxO) and cis-3-hexenylacetate (HxAC)) were obtained. Estimation methods were also used to predict each property which indicated that for oxygenated multifunctional compounds such as GLVs, a bond contribution method is more accurate than a group contribution method for predicting properties, but neither is recommended for complex, multifunctional compounds – especially those with substituted aromatic groups. If an experimentally determined value for either aqueous solubility or log(K_{OW}) is available, it is preferable to use it to correlate the other rather than using a "from scratch" method to estimate either. The effects on K_H of temperature and ionic strength relevant to natural fog water samples were found, yielding the enthalpy of phase change for each GLV and showing that all but four GLVs underwent a salting-out effect in the presence of aqueous phase ions. The surface to bulk aqueous and the air-surface partition coefficient were determined from the physico-chemical thermodynamic properties. This information was used in sample calculations to provide information on the partitioning characteristics of various compounds in natural water samples of different types, and was used to show that a sizable fraction of the GLV loading in an environmental fog droplet would be on the surface for all GLVs except MBO. Additionally, the scavenging efficiency as a function of the size of atmospheric water droplets can be obtained. From this, the amount of GLV in fog is shown to be significant, especially for MeJa. This is relevant for any aqueous media with large

surface area to volume ratios such as clouds and fog, and emphasizes the importance of aqueous phase photochemistry to fully elucidating SOA formation mechanisms. The physical properties determined in this study can be used in further studies and atmospheric multiphase models to determine the fate of GLVs in the atmosphere and their contribution to secondary organic aerosol production from the aqueous phase.

REFERENCES

Abraham, M. H., J. Andonian-Haftvan, G. S. Whiting, A. Leo and R. S. Taft (1994). "Hydrogen bonding. Part 34. The factors that influence the solubility of gases and vapours in water at 298 K, and a new method for its determination." Journal of the Chemical Society, Perkin Transactions 2(8): 1777-1791.

Arey, J., A. M. Winer, R. Atkinson, S. M. Aschmann, W. D. Long and C. L. Morrison (1991). "The emission of (Z)-3-hexen-1-ol, (Z)-3-hexenylacetate and other oxygenated hydrocarbons from agricultural plant species." Atmos. Environ., Part A **25A**(5-6): 1063-1075.

Ashworth, R. A., G. B. Howe, M. E. Mullins and T. N. Rogers (1988). "Air-water partitioning coefficients of organics in dilute aqueous solutions." Journal of Hazardous Materials **18**(1): 25-36.

Atkinson, R. (2000). "Atmospheric chemistry of VOCs and NOx." Atmos. Environ. **34**(12-14): 2063-2101.

Baev, A. K. (2012). Specific Intermolecular Interactions of Organic Compounds, Springer.

Bamford, H. A., D. L. Poster and J. E. Baker (1999). "Method for measuring the temperature dependence of the Henry's Law Constant of selected polycyclic aromatic hydrocarbons." Polycyclic Aromat. Compd. **14-15**: 11-22.

Banerjee, S., S. H. Yalkowsky and C. Valvani (1980). "Water solubility and octanol/water partition coefficients of organics. Limitations of the solubility-partition coefficient correlation." Environ. Sci. Technol. **14**(Copyright (C) 2014 American Chemical Society (ACS). All Rights Reserved.): 1227-1229.

Blando, J. D. and B. J. Turpin (2000). "Secondary organic aerosol formation in cloud and fog droplets: a literature evaluation of plausibility." Atmospheric Environment **34**(10): 1623-1632.

Cabani, S., P. Gianni, V. Mollica and L. Lepori (1981). "Group contributions to the thermodynamic properties of non-ionic organic solutes in dilute aqueous solution." Journal of Solution Chemistry **10**(8): 563-595.

Change, I. P. o. C. (2013). Contribution to the Fifth Assessment Report of the Intergovernmental Panel on Climate Change. T. F. Stocker and D. Qin.

Chen, J., F. S. Ehrenhauser, K. T. Valsaraj and M. J. Wornat (2006). "Uptake and UV-Photooxidation of Gas-Phase PAHs on the Surface of Atmospheric Water Films. 1. Naphthalene." J. Phys. Chem. A **110**(29): 9161-9168.

Chickos, J. S. and W. E. Acree (2003). "Enthalpies of Vaporization of Organic and Organometallic Compounds, 1880–2002." Journal of Physical and Chemical Reference Data **32**(2): 519-878.

Chin, M., R. Kahn and S. E. Schwartz (2009). Atmospheric Aerosol Properties and Climate Impacts., in U.S. Climate Change Science Program and the Subcommittee on Global Change Research. M. Chin, NASA.

Chiou, C. T., V. H. Freed, D. W. Schmedding and R. L. Kohnert (1977). "Partition coefficient and bioaccumulation of selected organic chemicals." Environ. Sci. Technol. **11**(Copyright (C) 2014 American Chemical Society (ACS). All Rights Reserved.): 475-478.

Chiou, C. T., D. W. Schmedding and M. Manes (1982). "Partitioning of organic compounds in octanol-water systems." Environ. Sci. Technol. **16**(1): 4-10.

Cramer, R. D. (1980). "BC(DEF) parameters. 2. An empirical structure-based scheme for the prediction of some physical properties." Journal of the American Chemical Society **102**(6): 1849-1859.

Dearden, J. C. and G. Schüürmann (2003). "Quantitative structure-property relationships for predicting henry's law constant from molecular structure." Environmental Toxicology and Chemistry **22**(8): 1755-1770.

Dewulf, J., D. Drijvers and H. van Langenhove (1995). "Measurement of Henry's law constant as function of temperature and salinity for the low temperature range." Atmos. Environ. **29**(3): 323-331.

EPA, U. from http://www.epa.gov/iaq/voc2.html.

EPA, U. (2012). Estimation Program Interface Suite. Washington, DC, US EPA.

Ervens, B., B. J. Turpin and R. J. Weber (2011). "Secondary organic aerosol formation in cloud droplets and aqueous particles (aqSOA): a review of laboratory, field and model studies." Atmos. Chem. Phys. **11**(21): 11069-11102.

Facchini, M. C., S. Decesari, M. Mircea, S. Fuzzi and G. Loglio (2000). "Surface tension of atmospheric wet aerosol and cloud/fog droplets in relation to their organic carbon content and chemical composition." Atmospheric Environment **34**(28): 4853-4857.

Falabella, J. B., A. Nair and A. S. Teja (2006). "Henry's Constants of 1-Alkanols and 2-Ketones in Salt Solutions." Journal of Chemical & Engineering Data **51**(5): 1940-1945.

Farag, M. A. and P. W. Pare (2002). "C6-Green leaf volatiles trigger local and systemic VOC emissions in tomato." Phytochemistry **61**(5): 545-554.

Fowler, D., K. Pilegaard, M. A. Sutton, P. Ambus, M. Raivonen, J. Duyzer, D. Simpson, H. Fagerli, S. Fuzzi, J. K. Schjoerring, C. Granier, A. Neftel, I. S. A. Isaksen, P. Laj, M. Maione, P. S. Monks, J. Burkhardt, U. Daemmgen, J. Neirynck, E. Personne, R. Wichink-Kruit, K. Butterbach-Bahl, C. Flechard, J. P. Tuovinen, M. Coyle, G. Gerosa, B. Loubet, N. Altimir, L. Gruenhage, C. Ammann, S. Cieslik, E. Paoletti, T. N. Mikkelsen, H. Ro-Poulsen, P. Cellier, J. N. Cape, L. Horvath, F. Loreto, U. Niinemets, P. Palmer, J. Rinne, P. Misztal, E. Nemitz, D. Nilsson, S. Pryor, M. W. Gallagher, T. Vesala, U. Skiba, N. Brueggemann, S. Zechmeister-Boltenstern, J. Williams, C. O'Dowd, M. C. Facchini, G. de Leeuw, A. Flossman, N. Chaumerliac, J. W. Erisman, D. Fowler, K. Pilegaard, M. A. Sutton, P. Ambus, M. Raivonen, J. Duyzer, D. Simpson, H. Fagerli, S. Fuzzi, J. K. Schjoerring, C. Granier, A. Neftel, I. S. A. Isaksen, P. Laj, M. Maione, P. S. Monks, J. Burkhardt, U. Daemmgen, J. Neirynck, E. Personne, R. Wichink-Kruit, K. Butterbach-Bahl, C. Flechard, J. P. Tuovinen, M. Coyle, G. Gerosa, B. Loubet, N. Altimir, L. Gruenhage, C. Ammann, S. Cieslik, E. Paoletti, T. N. Mikkelsen, H. Ro-Poulsen, P. Cellier, J. N. Cape, L. Horvath, F. Loreto, U. Niinemets, P. Palmer, J. Rinne, P. Misztal, E. Nemitz, D. Nilsson, S. Pryor, M. W. Gallagher, T. Vesala, U. Skiba, N. Brueggemann, S. Zechmeister-Boltenstern, J. Williams, C. O'Dowd, M. C. Facchini, G. de Leeuw, A. Flossman, N. Chaumerliac and J. W. Erisman (2009). "Atmospheric composition change: Ecosystems-Atmosphere interactions." Atmospheric Environment **43**(33): 5193-5267.

Gelencser, A. (2005). Carbonaceous Aerosol. Dordrecht, The Netherlands, Springer.

Goldstein, A. H. and I. E. Galbally (2007). "Known and unexplored organic constituents in the Earth's atmosphere." Environ. Sci. Technol. **41**(5): 1514-1521.

Graedel, T. E. (1978). Chemical Compounds in the Atmosphere. New York, Academic Press.

Graedel, T. E., Hawkins, D.T.; Claxton, L.D. (1986). Atmospheric Chemical Compounds. Orlando, FL, Academic Press.

Guenther, A., C. N. Hewitt, D. Erickson, R. Fall, C. Geron, T. Graedel, P. Harley, L. Klinger, M. Lerdau and a. et (1995). "A global model of natural volatile organic compound emissions." J. Geophys. Res., [Atmos.] **100**(D5): 8873-8892.

Hall, W. A. I. V. and M. V. Johnston (2010). "Oligomer content of α-pinene secondary organic aerosol." Aerosol Sci. Technol. **45**(1): 37-45.

Hallquist, M., J. C. Wenger, U. Baltensperger, Y. Rudich, D. Simpson, M. Claeys, J. Dommen, N. M. Donahue, C. George, A. H. Goldstein, J. F. Hamilton, H. Herrmann, T. Hoffmann, Y. Iinuma, M. Jang, M. E. Jenkin, J. L. Jimenez, A. Kiendler-Scharr,

W. Maenhaut, G. McFiggans, T. F. Mentel, A. Monod, A. S. H. Prévôt, J. H. Seinfeld, J. D. Surratt, R. Szmigielski and J. Wildt (2009). "The formation, properties and impact of secondary organic aerosol: current and emerging issues." Atmos. Chem. Phys. **9**(14): 5155-5236.

Hamilton, J. F., A. C. Lewis, T. J. Carey, J. C. Wenger, E. Borrais i Garcia and A. Munoz (2009). "Reactive oxidation products promote secondary volatile organic aerosol formation from green leaf volatiles." Atmospheric Chemistry and Physics **9**: 3815-3823.

Harley, P., V. Fridd-Stroud, J. Greenberg, A. Guenther and P. Vasconcellos (1998). "Emission of 2-methyl-3-buten-2-ol by pines: A potentially large natural source of reactive carbon to the atmosphere." Journal of Geophysical Research: Atmospheres **103**(D19): 25479-25486.

Harvey, R. M., J. Zahardis and G. A. Petrucci (2014). "Establishing the contribution of lawn mowing to atmospheric aerosol levels in American suburbs." Atmos. Chem. Phys. **14**(2): 797-812.

Heiden, A. C., T. Hoffmann, J. Kahl, D. Kley, D. Klockow, C. Langebartels, H. Mehlhorn, H. Sandermann, M. Schraudner, G. Schuh and J. Wildt (1999). "EMISSION OF VOLATILE ORGANIC COMPOUNDS FROM OZONE-EXPOSED PLANTS." Ecological Applications **9**(4): 1160-1167.

Herckes, P., K. T. Valsaraj and J. L. Collett, Jr. (2013). "A review of observations of organic matter in fogs and clouds: Origin, processing and fate." Atmos. Res. **132-133**: 434-449.

Hilal, S. H., S. W. Karickhoff and L. A. Carreira (2003). "Prediction of the vapor pressure, boiling point, heat of vaporization and diffusion coefficient of organic compounds." QSAR Comb. Sci. **22**(Copyright (C) 2014 American Chemical Society (ACS). All Rights Reserved.): 565-574.

Hine, J. and P. K. Mookerjee (1975). "Structural effects on rates and equilibriums. XIX. Intrinsic hydrophilic character of organic compounds. Correlations in terms of structural contributions." J. Org. Chem. **40**(Copyright (C) 2014 American Chemical Society (ACS). All Rights Reserved.): 292-298.

Ip, H. S. S., X. H. H. Huang and J. Z. Yu (2009). "Effective Henry's law constants of glyoxal, glyoxylic acid, and glycolic acid." Geophys. Res. Lett. **36**(1): L01802/01801-L01802/01805.

Isnard, P. and S. Lambert (1989). "Aqueous solubility and n-octanol/water partition coefficient correlations." Chemosphere **18**(9-10): 1837-1853.

Jain, N., Y. Ran and S. H. Yalkowsky (2001). "Prediction of Aqueous Solubility of Organic Compounds by the General Solubility Equation (GSE)." J. Chem. Inf. Comput. Sci. **41**(Copyright (C) 2014 American Chemical Society (ACS). All Rights Reserved.): 1208-1217.

Jardine, K., L. Abrell, S. A. Kurc, T. Huxman, J. Ortega and A. Guenther (2010). "Volatile organic compound emissions from Larrea tridentata (creosotebush)." Atmos. Chem. Phys. **10**(24): 12191-12206.

Kanakidou, M., J. H. Seinfeld, S. N. Pandis, I. Barnes, F. J. Dentener, M. C. Facchini, R. Van Dingenen, B. Ervens, A. Nenes, C. J. Nielsen, E. Swietlicki, J. P. Putaud, Y. Balkanski, S. Fuzzi, J. Horth, G. K. Moortgat, R. Winterhalter, C. E. L. Myhre, K. Tsigaridis, E. Vignati, E. G. Stephanou and J. Wilson (2005). "Organic aerosol and global climate modelling: a review." Atmos. Chem. Phys. **5**(4): 1053-1123.

Karl, T., A. Guenther, A. Turnipseed, E. G. Patton and K. Jardine (2008). "Chemical sensing of plant stress at the ecosystem scale." Biogeosciences **5**: 1287-1294.

Karl, T., C. Yeretzian, A. Jordan and W. Lindinger (2003). "Dynamic measurements of partition coefficients using proton-transfer-reaction mass spectrometry (PTR–MS)." International Journal of Mass Spectrometry **223–224**(0): 383-395.

Kesselmeier, J. and M. Staudt (1999). "Biogenic Volatile Organic Compounds (VOC): An Overview on Emission, Physiology and Ecology." Journal of Atmospheric Chemistry **33**(1): 23-88.

Kim, S., T. Karl, A. Guenther, G. Tyndall, J. Orlando, P. Harley, R. Rasmussen and E. Apel (2010). "Emissions and ambient distributions of Biogenic Volatile Organic Compounds (BVOC) in a ponderosa pine ecosystem: interpretation of PTR-MS mass spectra." Atmos. Chem. Phys. **10**(4): 1759-1771.

Kirstine, W., I. Galbally, Y. Ye and M. Hooper (1998). "Emissions of volatile organic compounds (primarily oxygenated species) from pasture." J. Geophys. Res., [Atmos.] **103**(D9): 10605-10619.

Liyana-Arachchi, T. P., A. K. Hansel, C. Stevens, F. S. Ehrenhauser, K. T. Valsaraj and F. R. Hung (2013). "Molecular Modeling of the Green Leaf Volatile Methyl Salicylate on Atmospheric Air/Water Interfaces." J. Phys. Chem. A **117**(Copyright (C) 2014 American Chemical Society (ACS). All Rights Reserved.): 4436-4443.

Liyana-Arachchi, T. P., C. Stevens, A. K. Hansel, F. S. Ehrenhauser, K. T. Valsaraj and F. R. Hung (2013). "Molecular simulations of green leaf volatiles and atmospheric oxidants on air/water interfaces." Phys. Chem. Chem. Phys. **15**(Copyright (C) 2014 American Chemical Society (ACS). All Rights Reserved.): 3583-3592.

Liyana-Arachchi, T. P., Z. Zhang, H. Vempati, A. K. Hansel, C. Stevens, A. T. Pham, F. S. Ehrenhauser, K. T. Valsaraj and F. R. Hung (2014). "Green Leaf Volatiles on Atmospheric Air/Water Interfaces: A Combined Experimental and Molecular Simulation Study." Journal of Chemical & Engineering Data.

Liyana-Arachchi, T. P., Z. Zhang, H. Vempati, A. K. Hansel, C. Stevens, A. T. Pham, F. S. Ehrenhauser, K. T. Valsaraj and F. R. Hung (2014). "Green Leaf Volatiles on Atmospheric Air/Water Interfaces: A Combined Experimental and Molecular Simulation Study." J. Chem. Eng. Data(Copyright (C) 2014 American Chemical Society (ACS). All Rights Reserved.): Ahead of Print.

Mackay, D., W. Y. Shiu and R. P. Sutherland (1979). "Determination of air-water Henry's law constants for hydrophobic pollutants." Environmental Science & Technology **13**(3): 333-337.

Marrero, J. and R. Gani (2002). "Group-Contribution-Based Estimation of Octanol/Water Partition Coefficient and Aqueous Solubility." Ind. Eng. Chem. Res. **41**(Copyright (C) 2014 American Chemical Society (ACS). All Rights Reserved.): 6623-6633.

Matsui, K. (2006). "Green leaf volatiles: hydroperoxide lyase pathway of oxylipin metabolism." Current Opinion in Plant Biology **9**(3): 274-280.

Mauderly, J. L. and J. C. Chow (2008). "Health Effects of Organic Aerosols." Inhalation Toxicol. **20**(3): 257-288.

Mentel, T. F., E. Kleist, S. Andres, M. Dal Maso, T. Hohaus, A. Kiendler-Scharr, Y. Rudich, M. Springer, R. Tillmann, R. Uerlings, A. Wahner and J. Wildt (2013). "Secondary aerosol formation from stress-induced biogenic emissions and possible climate feedbacks." Atmos. Chem.Phys. **13**: 8755-8770.

Meylan, W. M. and P. H. Howard (1991). "Bond contribution method for estimating henry's law constants." Environmental Toxicology and Chemistry **10**(10): 1283-1293.

Meylan, W. M. and P. H. Howard (1995). "Atom/Fragment Contribution Method for Estimating Octanol-Water Partition Coefficients." J. Pharm. Sci. **84**(1): 83-92.

Meylan, W. M. and P. H. Howard (1996). Sources and estimations of octanol-water partition coefficients and water solubilities, Lewis.

Miller, M. M., S. P. Wasik, G. L. Huang, W. Y. Shiu and D. Mackay (1985). "Relationships between octanol-water partition coefficient and aqueous solubility." Environmental Science & Technology **19**(6): 522-529.

Mmereki, B. T. and D. J. Donaldson (2003). "Direct observation of the kinetics of an atmospherically important reaction at the air-aqueous interface." J. Phys. Chem. A

107(Copyright (C) 2014 American Chemical Society (ACS). All Rights Reserved.): 11038-11042.

Modarresi, H., H. Modarress and J. C. Dearden (2007). "QSPR model of Henry's law constant for a diverse set of organic chemicals based on genetic algorithm-radial basis function network approach." Chemosphere **66**(11): 2067-2076.

Morawetz, E. (1972). "Enthalpies of vaporization for a number of aromatic compounds." The Journal of Chemical Thermodynamics **4**(3): 455-460.

Munger, J. W., D. J. Jacob, J. M. Waldman and M. R. Hoffmann (1983). "Fogwater chemistry in an urban atmosphere." JGR, J. Geophys. Res., [Sect.] C **88**(C9): 5109-5121.

Nirmalakhandan, N., R. A. Brennan and R. E. Speece (1997). "Predicting Henry's law constant and the effect of temperature on Henry's law constant." Water Res. **31**(Copyright (C) 2014 American Chemical Society (ACS). All Rights Reserved.): 1471-1481.

Preston, C. A., G. Laue and I. T. Baldwin (2001). "Methyl jasmonate is blowing in the wind, but can it act as a plant–plant airborne signal?" Biochemical Systematics and Ecology **29**(10): 1007-1023.

Pruppacher, H. R. and R. Jaenicke (1995). "The processing of water vapor and aerosols by atmospheric clouds, a global estimate." Atmospheric Research **38**(1–4): 283-295.

Raja, S., R. Raghunathan, R. R. Kommalapati, X. Shen, J. L. Collett and K. T. Valsaraj (2009). "Organic composition of fogwater in the Texas-Louisiana gulf coast corridor." Atmos. Environ. **43**(27): 4214-4222.

Raja, S., R. Ravikrishna, R. R. Kommalapati and K. T. Valsaraj (2005). "Monitoring of fogwater chemistry in the gulf coast urban industrial corridor: Baton Rouge (louisiana)." Environ Monit Assess **110**(1-3): 99-120.

Richards-Henderson, N. K., A. K. Hansel, K. T. Valsaraj and C. Anastasio (2014). "Aqueous oxidation of green leaf volatiles by hydroxyl radical as a source of SOA: Kinetics and SOA yields." Atmos. Environ. **95**: 105-112.

Robinson, A. L., N. M. Donahue, M. K. Shrivastava, E. A. Weitkamp, A. M. Sage, A. P. Grieshop, T. E. Lane, J. R. Pierce and S. N. Pandis (2007). "Rethinking Organic Aerosols: Semivolatile Emissions and Photochemical Aging." Science (Washington, DC, U. S.) **315**(5816): 1259-1262.

Russell, C. J., S. L. Dixon and P. C. Jurs (1992). "Computer-assisted study of the relationship between molecular structure and Henry's law constant." Analytical Chemistry **64**(13): 1350-1355.

Schüürmann, G. (1995). "Quantum chemical approach to estimate physicochemical compound properties: Application to substituted benzenes." Environmental Toxicology and Chemistry **14**(12): 2067-2076.

Seinfeld, J. H. and S. N. Pandis (1998). Atmospheric Chemistry and Physics: From Air Pollution to Climate Change, Wiley.

Seinfeld, J. H., S. N. Pandis and Editors (2006). Atmospheric chemistry and physics: from air pollution to climate change, 2nd Edition, Wiley.

Shiojiri, K., K. Kishimoto, R. Ozawa, S. Kugimiya, S. Urashimo, G. Arimura, J. Horiuchi, T. Nishioka, K. Matsui and J. Takabayashi (2006). "Changing green leaf volatile biosynthesis in plants: An approach for improving plant resistance against both herbivores and pathogens." Proceedings of the National Academy of Sciences of the United States of America **103**(45): 16672-16676.

Staudinger, J. and P. V. Roberts (1996). "A critical review of Henry's law constants for environmental applications." Crit. Rev. Environ. Sci. Technol. **26**(Copyright (C) 2014 American Chemical Society (ACS). All Rights Reserved.): 205-297.

Suzuki, T., K. Ohtaguchi and K. Koide (1992). "Application of principal components analysis to calculate Henry's constant from molecular structure." Comput. Chem. **16**(Copyright (C) 2014 American Chemical Society (ACS). All Rights Reserved.): 41-52.

Tewari, Y. B., M. M. Miller, S. P. Wasik and D. E. Martire (1982). "Aqueous solubility and octanol/water partition coefficient of organic compounds at 25.0°C." J. Chem. Eng. Data **27**(Copyright (C) 2014 American Chemical Society (ACS). All Rights Reserved.): 451-454.

Torres-Gómez, L. A., G. Barreiro-Rodríguez and A. Galarza-Mondragón (1988). "A new method for the measurement of enthalpies of sublimation using differential scanning calorimetry." Thermochimica Acta **124**(0): 229-233.

Valsaraj, K. T. (2004). "Adsorption of polycyclic aromatic hydrocarbons at the air-water interface and its role in atmospheric deposition by fog droplets." Environ Toxicol Chem **23**(10): 2318-2323.

Valsaraj, K. T. (2009). Elements of environmental engineering : thermodynamics and kinetics. Boca Raton, CRC Press.

Valsaraj, K. T. (2012). "A review of the aqueous aerosol surface chemistry in the atmospheric context." Open J. Phys. Chem. **2**(1): 58-66.

Volkamer, R., J. L. Jimenez, F. San Martini, K. Dzepina, Q. Zhang, D. Salcedo, L. T. Molina, D. R. Worsnop and M. J. Molina (2006). "Secondary organic aerosol

formation from anthropogenic air pollution: rapid and higher than expected." Geophys. Res. Lett. **33**(17): L17811/17811-L17811/17814.

Wadia, Y., D. J. Tobias, R. Stafford and B. J. Finlayson-Pitts (2000). "Real-Time Monitoring of the Kinetics and Gas-Phase Products of the Reaction of Ozone with an Unsaturated Phospholipid at the Air-Water Interface." Langmuir **16**(Copyright (C) 2014 American Chemical Society (ACS). All Rights Reserved.): 9321-9330.

Williams, J., U. Pöschl, P. J. Crutzen, A. Hansel, R. Holzinger, C. Warneke, W. Lindinger and J. Lelieveld (2001). "An Atmospheric Chemistry Interpretation of Mass Scans Obtained from a Proton Transfer Mass Spectrometer Flown over the Tropical Rainforest of Surinam." Journal of Atmospheric Chemistry **38**(2): 133-166.

APPENDIX

Appendix A. Derivation of Thermodynamic Equations

The Henry's Constant of a compound can be defined in varying units, here it is defined as $K_H = C_W/P$ [=] [M/atm], where C_W is the analyte's concentration in the aqueous phase, and P is its partial pressure in the gas phase. It was originally an empirical result reflecting the observation that amount gas dissolved in a liquid at equilibrium is proportional to its partial pressure in equilibrium. In order to understand the use and potential estimations of Henry's Constant, solubility, and log(K_{OW}) it is important to have some thermodynamic background. In mixed solutions at equilibrium with air above it, the fugacity $\hat{f}$ of an analyte in each phase are equal.

$$\hat{f}_G = \hat{f}_L \tag{7}$$

Here $\hat{f}_G$ is the analyte's fugacity in the gas phase and $\hat{f}_L$ is its fugacity in the liquid phase. If ideality in the gas phase is assumed then $\hat{f}_G$ is equal to the analyte's partial pressure P and Equation 7 can be expanded to Equation 8.

$$P = f_L * \gamma_L * x_L \tag{8}$$

Here f_L is the reference liquid fugacity, γ_L is the analyte fugacity in the liquid phase, and x_L is the anlyte's liquid phase mol fraction. If we substitute the relation $x_L = C_L * \bar{V}_L$ where $\bar{V}_L$ is the molar volume of the solution and C_L is the analyte's concentration in it. By using Henry's Law conventions (as C_L goes to zero, γ_L becomes 1), and if the solution is assumed sufficiently dilute then this allows us to write:

$$\lim_{C_L \to 0} \left(\frac{P}{C_L}\right) = f_L * \gamma_L * \bar{V}_L = K_H \tag{9}$$

If the liquid is taken to be water, this is the definition of Henry's Law, and the one I will be using in this work.

The saturated aqueous solubility of an analyte can likewise be expressed in fugacity terms by equating the fugacity of the compound in its pure state with that of the compound in a saturated aqueous state. This is shown below:

$$f_P * \gamma_P * x_P = f_P * \gamma_W * x_W \quad (10)$$

where the subscript P stands for the pure component state and W for the aqueous state. The reference liquid state is taken to be the pure liquid solute, and these pure component fugacities cancel out. Additionally for the pure component phase $\gamma_P = x_P = 1$, and by substituting $x_W = C_W * \bar{V}_W$ we find the final relation.

$$\gamma_W = (C_W * \bar{V}_W)^{-1} = (S * \bar{V}_W)^{-1} \quad (11)$$

Equation 9 states that the activity coefficient for an analyte in a saturated aqueous solution is inversely proportional to its saturated aqueous concentration.

The octanol-water partitioning of an analyte can also be expressed in terms of fugacity. In an octanol-water system at equilibrium, the fugacity of the analyte in the octanol phase (designated by subscript O) is equal to the fugacity of the analyte in the aqueous phase (designated by subscript W), and if the reference fugacity is again that of the pure component liquid, we find Equation 12.

$$f_P * \gamma_O * x_O = f_P * \gamma_W * x_W \quad (12)$$

The pure component reference fugacity values again cancel, and if one substitutes $x_O = C_O * \bar{V}_O$, then by using the definition of octanol-water partition coefficient $K_{OW} = C_O/C_W$, Equation 13 is found.

$$K_{OW} = \frac{C_O}{C_W} = \frac{\gamma_W * \bar{V}_W}{\gamma_O * \bar{V}_O} \quad (13)$$

This can be correlated to the aqueous solubility of an analyte by substituting in the γ^w relation found in Equation 8. This gives the result that K_{OW} is proportional to inverse of the aqueous solubility, which by taking the logarithm can also be expressed:

$$\log K_{OW} = -\log S - \log(\gamma_O * \bar{V}_O) \quad (14)$$

Thus a linear relationship between log(K_{OW}) and log(S) with slope -1 is found. However, this neglects the fact that the solvents are not pure octanol and pure water, but are well mixed at equilibrium and thus are mutually saturated. These changes are reflected in Equation 15, the expression for K_{OW}.

$$K_{ow} = \frac{c^o}{c^w} = \frac{\gamma'_W * \bar{V}_W^*}{\gamma'_O * \bar{V}_O^*} \quad (15)$$

Here γ'_W and γ'_O are the compound's activity coefficient in mutually saturated water and octanol respectively. $\bar{V}_W^*$ and $\bar{V}_O^*$ are the molar volume for the mutually saturated water and octanol phases respectively. $\bar{V}_W^*$ is approximately equal to $\bar{V}_W$ (Miller et al. 1985), allowing combination with Equation 9. This eventually leads to Equation 14.

$$\log K_{OW} = -\log S + \log \gamma'_W - \log(\gamma'_O * \gamma'_W * \bar{V}_O^*) \quad (16)$$

These relationships form the thermodynamic basis of the log(K_{OW}) vs log(S) correlation.

Appendix B. Tables of estimations of physico-chemical properties for GLVs

Table 8. Estimated Henry's Constants for each GLV [$M \cdot atm^{-1}$]

GLV	Measured (Current Study)	HENRYWIN Bond (Meylan and Howard 1991)	HENRYWIN Group (Hine and Mookerjee 1975)	Hine & Mookerjee (Hine and Mookerjee 1975)	Suzuki et al. (Suzuki et al. 1992)	Nirmalakhandan & Speece (Nirmalakhandan et al. 1997)	SPARC (Hilal et al. 2003)
MeJa	8091 ± 1121	2267.57	72463.77	4385.00	2827.50	176.73	4365.16
MeSa	37.9 ± 2.1	219.78	448430.49	20510.20	522473.53	180783.25	933.25
MBO	52.9 ± 5.1	101.21	Incomplete	264.22	187.32	176.83	70.79
HxO	113 ± 15	64.52	195.69	81.65	187.41	240.82	144.54
HxAC	3.60 ± 0.22	1.57	6.06	2.70	0.78	7.24	3.02

Table 9. Estimated ln(Solubility [mM]) for each GLV

GLV	Measured (Current Study)	Marrero & Gani (Marrero and Gani 2002)	WATERNT (Meylan and Howard 1995)	WSKOW (Meylan and Howard 1996)	SPARC (Hilal et al. 2003)	Chiou et al. (Chiou et al. 1977)	Jain et al. (Jain et al. 2001)	Isnard & Lambert (Isnard and Lambert 1989)	Banerjee et al. (Banerjee et al. 1980)
MeJa	1.51	-1.22	0.41	0.34	1.63	1.51	2.19	1.7269	2.07
MeSa	1.64	3.98	3.33	2.51	2.97	2.17	2.62	2.3703	2.71
MBO	7.55	5.43	6.42	7.11	6.38	7.90	6.47	8.0252	8.36
HxO	5.08	3.56	5.04	5.25	4.31	5.05	4.56	5.2147	5.55
HxAC	1.14	1.57	1.94	1.48	1.50	1.75	2.35	1.9640	2.30

Table 10. Estimated log(K_{OW}) values for each GLV

GLV	Measured	KOWWIN (Meylan and Howard 1995)	Marrero & Gani (Marrero and Gani 2002)	SPARC (Hilal et al. 2003)	Meylan & Howard (Meylan and Howard 1996)	Chiou et al. (Chiou et al. 1977)	Jain et al. (Jain et al. 2001)	Isnard & Lambert (Isnard and Lambert 1989)	Banerjee et al. (Banerjee et al. 1980)
MeJa	2.55	2.76	2.58	2.72	1.77	1.51	2.19	2.61	2.71
MeSa	2.36	2.60	1.61	1.59	2.99	2.17	2.62	2.58	2.68
MBO	0.69	1.08	1.22	1.14	0.47	7.90	6.47	0.83	0.93
HxO	1.52	1.61	1.22	1.87	1.60	5.05	4.56	1.56	1.66
HxAC	2.48	2.61	2.42	2.76	2.65	1.75	2.35	2.72	2.82

VITA

Harsha Satyanarayana Vempati was raised in Chandler, Arizona and graduated from Corona del Sol High School in 2008. Afterwards, he moved to Atlanta, Georgia and received his bachelor's degree at the Georgia Institute of Technology in 2012. He was interested in environmental sciences, and upon acceptance into Louisiana State University's Cain Department of Chemical Engineering, joined the chemodynamics laboratory. He will receive his degree in December 2014, and upon completion plans to work as an environmental consultant.